
**~~An~~Palynological evidence reveals an arid early Holocene—revealed by
palynological evidence for the north-east Tibetan Plateau**

Nannan Wang^{1,2}, Lina Liu^{1,2}, Xiaohuan Hou¹, Yanrong Zhang¹, Haicheng Wei³, Xianyong Cao^{1*}

¹ Alpine Paleoecology and Human Adaptation Group (ALPHA), State Key Laboratory of Tibetan Plateau Earth System, Resources and Environment (TPESRE), Institute of Tibetan Plateau Research, Chinese Academy of Sciences, Beijing 100101, China

² University of the Chinese Academy of Sciences, Beijing 100049, China

³ Key Laboratory of Comprehensive and Highly Efficient Utilization of Salt Lake Resources, Qinghai Institute of Salt Lakes, Chinese Academy of Sciences, Xining 810008, China

Correspondence to: Xianyong Cao (xcao@itpcas.ac.cn)

Abstract. Situated ~~in~~within the triangle of the East Asian monsoon, the Indian monsoon, and the westerlies, the Holocene patterns of climate and vegetation changes on the north-east Tibetan Plateau are still unclear or even contradictory. By investigating the distribution of modern pollen taxa on the east Tibetan Plateau, we infer the past vegetation and climate since ~~the last~~ 14.2 ka BP (thousand years before present) from a fossil pollen record extracted from Gahai Lake (102.3133°E, 34.2398°N; 3444 m a.s.l.) together with multiple proxies (grain-size, contents of total organic carbon and total nitrogen) on the north-east Tibetan Plateau. Results indicate that the Gahai Basin was covered by arid alpine steppe or even desert between 14.2 and 7.4 ka BP with ~~a mild and~~ dry ~~climate~~climatic conditions, and high percentages of ~~arboreous~~arboreal pollen are thought to be long-distance wind transported grains. Montane forest (dominated by *Abies*, *Picea*, and *Pinus*) migrated into the Gahai Basin between 7.4 and 3.8 ka BP driven by wet and warm climatic conditions (the climate optimum within the Holocene) but reverted to alpine steppe between 3.8 and 2.3 ka BP, indicating a drying climate trend. After 2.3 ka BP, vegetation shifted to alpine meadow represented by increasing abundances of Cyperaceae, which may reflect a cooling climate. The strange pollen spectra with high abundances of Cyperaceae and

high total pollen concentrations after ca. 0.24 ka BP (1710 CE) could be an indication of disturbance by human activities to some extent, but needs more direct evidence to be confirmed. Our study confirms the occurrence of a climate optimum in the mid-Holocene on the north-east Tibetan Plateau, which is consistent with climate records from the fringe areas of the East Asian summer monsoon, and provides new ~~insight~~insights into the ~~evolution~~fluctuations in the intensity and extent of the Asian monsoon system.

Keywords: Gahai Lake; pollen; climate reconstruction; vegetation evolution; last deglacial

1 Introduction

Vegetation, as an essential component in the terrestrial ecosystem, responds to and represents well environmental and climatic changes~~-well~~. Investigating the patterns and mechanisms of past vegetation changes ~~can provide~~provides a reliable analogue for predicting future climate and vegetation changes (Mykleby et al., 2017; Zhao et al., 2017). Since the sharp climate warming during the last deglacial (after ca. 15 ka BP in the Northern Hemisphere; Wang et al., 2001; Andersen et al., 2004; Dykoski et al., 2005; Xu et al., 2013), the response of vegetation to climate warming could be a valuable palaeo-analogue for understanding current vegetation changes under global warming and for predicting future vegetation trends (Birks, 2019).

The north-east Tibetan Plateau lies in the transition between the East Asian summer monsoon, the Indian summer monsoon, and the westerlies;~~it~~is sensitive to climate change₂ and is an ideal region to study past vegetation and climate variation (Bryson, 1986; An et al., 2012; Chen et al., 2016). Nevertheless, the climate records from different lacustrine sediments on the north-east Tibetan Plateau show a lack of consistency, for example, regarding the climatic conditions during the early Holocene. Some records reveal that the climate was relatively dry on the north-east Tibetan Plateau and controlled by the East Asian monsoon during the early Holocene (Shen et al., 2005; Herzsuh et al., 2006; Cheng et al., 2013), while other records such as

those from Hala Lake and Genggahai Lake show that there was maximum water depth and hence a climatic optimum in the early Holocene (Qiang et al., 2013; Yan and Wünnemann, 2014; Wang et al., 2021). Therefore, more studies are needed to clarify the early Holocene climatic conditions, which are necessary to resolve the environmental evolution of the north-east Tibetan Plateau.

Pollen plays an important role in reconstructing the past vegetation and climate owing to its preservation in various sediment types (Chevalier et al., 2020). However, pollen-based vegetation and climate reconstructions on the Tibetan Plateau are also confronted with challenges, for instance, the current quantitative reconstructions of vegetation and climate are based on pollen percentages, which can be biased when there is much exogenous arboreal pollen, especially in strata with extremely low pollen concentrations because the exogenous arboreal pollen will enlarge its form a larger proportion in of the pollen spectra sample (Herzschuh, 2007; Ma et al., 2017; 2019). Exogenous arboreal pollen can be recognised in areas far away from forested regions, mainly because no trees grow around the lake or its adjacent areas nowadays, such as Luanhaizi Lake (Herzschuh et al., 2010), Donggi Cona Lake (Wang et al., 2014), ~~Hala Lake (Hu et al., 2016)~~, and Kuhai Lake (Wischnewski et al., 2011). Arboreal pollen can then be excluded in subsequent analysis to ensure the correct interpretation of vegetation and environment. However, it is somewhat difficult to recognise the contribution of exogenous pollen from areas near the forest on the eastern part of the Tibetan Plateau, which could seriously impact the results of pollen reconstruction vegetation reconstructions, such as from Naleng Lake (Kramer et al., ~~2010a~~ 2010) and Qinghai Lake (Shen et al., 2005). Solving this issue of clarifying the influence of exogenous pollen is an important prerequisite for a better understanding of the early Holocene climate shifts. Understanding the spatial distribution characteristics of modern pollen and their relationships may be an effective way to identify such arboreal pollen properties.

In this study, we integrate multi-proxy records (pollen, grain size, total organic carbon (TOC), total nitrogen (TN)) of Gahai Lake to reconstruct the climate and vegetation

evolution since the last deglacial. We assess the dispersal ability and biotopes of the main pollen taxa in the pollen record by investigating the distribution of modern pollen and their relationship with climate. We attempt to recognise exogenous pollen and evaluate its influence on reconstruction results to determine whether the early Holocene of the north-east Tibetan Plateau was dry or wet.

2 Study area

Gahai Lake (102.3133°E, 34.2398°N; 3444 m a.s.l.) is situated in the upper reaches of the Yellow River on the north-east Tibetan Plateau, a transitional zone between the Tibetan Plateau, the mountainous area of Longnan, and the Loess Plateau (Fig. 1).

Gahai Lake is a typical plateau interior freshwater lake, with a total area of 15 km² and a mean water depth ranging from 2 to 2.5 m. The water supply of the lake is mainly from precipitation, groundwater recharge, and surface runoff from surrounding mountains to the south and south-east including Qiongmuequ, Wenniqu, and Geqiongkuhe rivers, and there is a single outflow stream at the north-western end of the basin (Duan et al., 2016; Fig. 1). Gahai Lake currently belongs to the alpine humid climate zone, which is influenced by the West Pacific Subtropical High in summer and controlled by westerlies in winter. Climate characteristics are rain in the warm season, and large seasonal and diurnal temperature differences (Liang, 2006). Mean annual temperature of this region is 1.2°C and mean annual precipitation is 782 mm, with about 80% of precipitation falling in the rainy season (from June to September), and mean annual evaporation is 1150 mm (Duan et al., 2016).

Vegetation cover in Gahai Basin exceeds 90%. There are abundant species in the grassland community, which is at the intersection ~~between~~of various flora, and perennial herbs predominate. The dominant plant species include *Poa annua*, *Carex*, *Clintoniaudensis*, *Polygonum*, *Ranunculus japonicus*, *Potentilla fruticosa*, *Neyraudia reynaudiana*, and *Elymus nutans*. Forest is found in the eastern low mountains with a mosaic distribution of meadow and shrub, dominated by *Abies*, *Picea*, *Betula*, and Cupressaceae. *Picea* is found in damp areas at the foot of mountains and replaced by

Betula as a transitional community after being cut down; *Abies* occurs on shady and semi-shady slopes between 3200 and 3400 m a.s.l.; Cupressaceae is distributed mostly on sunny and semi-sunny slopes of more than 35 degrees. This region belongs to a typical stockbreeding district, and the grazing activity focuses on the grassland. In addition, there is small-scale ~~agricultural~~agriculture along the river valley at low elevations (Liang et al., 2006; Duan et al., 2016).

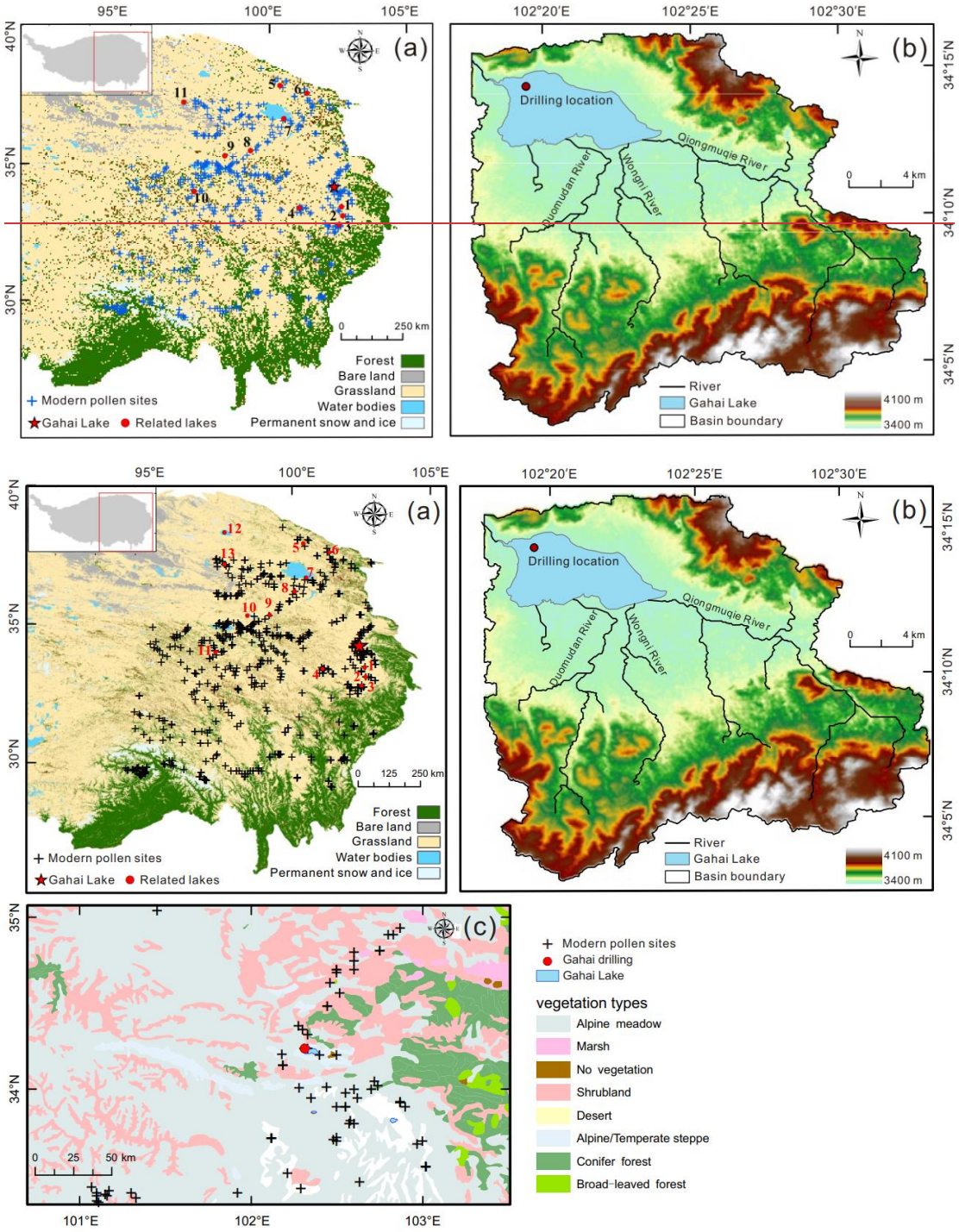


Figure 1. (a) ~~Land-use map~~The locations of the ~~eastern Tibetan Plateau~~related lakes and modern surface samples (Du, 2019). Lakes referred to in the text: 1, ZB08-C1; 2, ZB10-C14; 3, Hongyuan peatland; 4, Ximencuo Lake; 5, Dalianhai Lake; 6, Luanhaizi Lake; 7, Qinghai Lake; 8, Genggahai Lake; 9, Kuhai Lake; ~~910~~, Donggi Cona Lake; ~~4011~~, Koucha Lake; ~~11, Hurleg Lake~~; ~~12, Hala Lake~~; 13, Gahai Lake (Qaidam basin). (b) Catchment map and coring site of Gahai Lake. (c) Distribution of modern pollen samples in the vicinity of Gahai Lake.

3 Material and methods

3.1 Modern pollen data and their climate data

Our modern pollen dataset (n=731) is derived from the east Tibetan Plateau ranging from 94.07 to 103.02°E and from 29.13 to 38.48°N, with elevations from 2515 to 5008 m a.s.l. These modern pollen data are mainly from the modern pollen database of China and Mongolia (Cao et al., 2014) and recently published pollen data for the east Tibetan Plateau (Cao et al., 2021; Wang et al., 2022). The pollen sites are generally evenly distributed across the east Tibetan Plateau, covering subalpine forest, alpine meadow, alpine steppe, and alpine desert (Fig. 1). Pollen sample types include topsoil, lake surface-sediments, and moss polsters mainly.

We selected four important climate variables including mean annual precipitation (P_{ann}), mean temperature of the warmest month (Mt_{wa}), mean temperature of the coldest month (Mt_{co}), and mean annual temperature (T_{ann}), together with elevation (Elev) to investigate the relationship between pollen assemblages and ~~environment following previous studies (Lu et al., 2011; Herzschuh~~the environment because these are important factors influencing the pollen distribution on the Tibetan Plateau (Lu et al., 2011; Cao et al., 2021; Wang et al., 2022). Modern climatic data were obtained from the Chinese Meteorological Forcing Dataset (CMFD; gridded near-surface meteorological dataset), and each sample is assigned to the nearest pixel of the CMFD using the *fields* package version 13.3 (Nychka et al., 2021) of R (version 4.0.3; R Core Team, 2021). The detailed processes of obtaining climatic data are presented in ~~the~~ Fig. A1.

3.2 Sediment sampling and radiocarbon dating

A 329-cm-long sediment core (named GAH) was obtained using a UWITEC platform from the deepest part of Gahai Lake (ca. 2 m) in January 2019 (Fig. 1), and then transported to the Institute of the Tibetan Plateau Research for preservation. GAH was sub-sampled at 1 cm intervals, and all sub-samples were freeze-dried.

The age-depth model for GAH was established by ^{210}Pb , ^{137}Cs , and accelerator mass spectrometry (AMS) radiocarbon dating. The top 20 cm of the sediment at 1-cm intervals was measured for ^{210}Pb and ^{137}Cs at the School of Geographical Science, Nantong University. The constant rate of supply (CRS) model was selected to calculate the dates due to the non-monotonic variation of unsupported ^{210}Pb activity, as the results revealed that the ^{210}Pb dates were inconsistent with the ^{137}Cs peak of 1963 CE (Appleby, 2001). To solve this problem, the core was divided into two sections using $^{210}\text{Pb}_{\text{ex}}$ activity variation data using different formulae to calculate the dates and obtain a good effect. Finally, an age-depth model based on a ^{210}Pb -CRS model corrected by ^{137}Cs peak was generated (Fig. 4a). ~~Twelve~~Thirteen bulk organic sediment samples of 1-cm thickness were sent for AMS ^{14}C dating by Beta Analytic Inc., USA, owing to a lack of macrofossils (Table 2). The age-depth model was established using the Bayesian age-depth ~~modelling~~modeling in the *rbacon* package (version 2.5.7; Blaauw and Christen 2011; Blaauw et al., 2021) in R (R Core Team 2021) and the IntCal20 radiocarbon calibration curve (Reimer et al., 2020).

3.3 Laboratory analysis

The pollen samples (0.6–22 g; $n=111$; at 1 to 2 cm intervals) were treated with hydrofluoric acid sieving-analysis (Fægri and Iversen, 1975). *Lycopodium* spores (ca. 27,560 grains) were added to the samples to calculate the pollen concentration, then samples were processed with 10% HCl, 10% KOH, and 36% HF, and sieved through a 7 μm nylon mesh, followed by acetolysis (9:1 mixture of acetic anhydride and sulphuric acid) treatment. Finally, glycerin was added to preserve the samples. The pollen taxa were identified and counted with a 400x LEICA DM 2500 optical

microscope, with the aid of modern pollen reference slides collected from the eastern and central Tibetan Plateau (including 401 common species of alpine meadow; Cao et al., 2020) and published atlases for pollen and spores (Wang et al., 1995; Tang et al., 2017). At least 100 terrestrial pollen grains were counted for most samples, except for 10 samples owing to extremely low pollen concentration; and more than 3000 *Lycopodium* spores were counted for each sample ~~above 176 cm, which could reflect~~ the palaeo-vegetation at that time. Because of the low pollen concentrations below the depth 176 cm, only pollen data for the upper part of the core are presented and discussed.

For the grain-size analysis, freeze-dried samples (1 g; $n=176$; above 176 cm) were treated with 30% H_2O_2 to remove organic matter and 10% HCl to remove carbonate, cleaned with deionized water and kept stable for 24 h, before adding 0.5 N sodium hexametaphosphate (10 ml) and undergoing ultrasonic cleaning for 10 minutes. A laser diffraction particle size analyser MASTERSIZER 3000 (Chen et al., 2013) was used, with each sample being tested 3 times and their average value used in the final grain-size data.

A total of 176 samples were analysed to obtain organic matter change since the last deglacial, including TN and TOC. Catalysts were added to freeze-dried samples and reacted quickly. TN was measured with an Elementar element analyser (CNS analyser, Vario MAX Cube)/Elementar Vario EL III which has a measurement accuracy of 0.001. TOC was measured with a Vario MAX C analyser, and has the same accuracy as TN. All samples were ground to ensure sufficient reaction before testing. The C/N ratio was calculated by dividing TOC by TN.

3.4 Numerical analyses

Ordination analyses were employed to investigate the modern relationship between pollen taxa and climatic variables for the eastern Tibetan Plateau. Pollen taxa (with $\geq 10\%$ maximum and ≥ 30 occurrences) from the 731 modern pollen assemblages were used for detrended correspondence analysis (DCA; Hill and Gauch, 1980). The length

of the first axis of the pollen data was 3.29 SD (standard deviation units), indicating that a linear response model is suitable for the modern pollen dataset (ter Braak and Verdonschot, 1995). Hence, we performed redundancy analysis (RDA) to visualise the distribution of pollen species and sampling sites along the climatic gradients. We used the variance inflation factor (VIF) to determine high collinearities within the model, and stopped adding variables to ensure all VIF values are lower than 20 (ter Braak and Prentice, 1988; Table 1). All ordination analyses were run using the *rda* function in the *rioja* package version 0.9–26 (Oksanen et al., 2019; Juggins, 2020) in R, using square-root transformed modern pollen percentages to optimise the signal-to-noise ratio (Prentice, 1980).

For the fossil pollen dataset obtained from GAH, 22 pollen taxa (those present in at least 3 samples and with a $\geq 3\%$ maximum) with square-root transformed percentages were selected for ordination analyses. The length of the first axis was 1.67 SD, indicating a principal component analysis (PCA) is suitable to investigate the relationship between the pollen taxa. PCA was run using the *rda* function in the *vegan* package (version 2.5-4; Oksanen et al., 2019) in R.

In addition, weighted-averaging partial least squares (WA-PLS) was employed to establish a pollen–climate transfer function using the modern pollen dataset, and to quantitatively reconstruct past climate for the GAH pollen record. More details of the reconstruction are presented in the Supplement.

Table 1. Summary statistics for redundancy analysis (RDA) with 19 pollen taxa and four climate variables. VIF: variance inflation factor; P_{ann} : mean annual precipitation (mm); Mt_{co} : mean temperature of the coldest month ($^{\circ}\text{C}$); Mt_{wa} : mean temperature of the warmest month ($^{\circ}\text{C}$); T_{ann} : mean annual temperature ($^{\circ}\text{C}$); and Elev: elevation (m a.s.l).

Climate variables	VIF (without T_{ann})	VIF (add T_{ann})	Climate variables as sole predictor	Marginal contribution based on climate variables	
			Explained variance (%)	Explained variance (%)	<i>p</i> -value
P_{ann}	3.0	3.1	5.2	7.1	0.001
Mt_{co}	4.5	133.6	4.9	0.3	0.001
Mt_{wa}	6.5	111.7	3.7	5.7	0.001
Elev	2.5	3.0	4.5	0.2	0.001
T_{ann}	-	403.9	-	-	-

4 Results

4.1 Relationships of pollen taxa to climatic variables and elevation

The modern pollen dataset for the east Tibetan Plateau contains 107 pollen taxa and covers a long P_{ann} gradient (161–963 mm) and broad Mt_{wa} gradient (1.8–18.5 °C) (Fig. 2; A1). High abundances of arboreal pollen taxa ~~occur in areas with warm and wet climate, for instance, including~~ *Abies*, *Quercus* (evergreen, E), *Corylus*, and *Carpinus* are mainly distributed in regions with ~~high~~- P_{ann} higher than 450 mm and Mt_{co} higher than -15 °C (Fig. 2; A1). ~~Although high abundances of~~ *Pinus*, (up to 2.3%, mean 0.3%), *Picea*, (up to 25.7%, mean 0.5%), and *Betula* (up to 5.7%, mean 0.4%) are also ~~restricted to warm and wet areas, they are~~ widely distributed and appear ~~even~~ in extreme ~~drought~~dry and cold sampling sites where P_{ann} is lower than

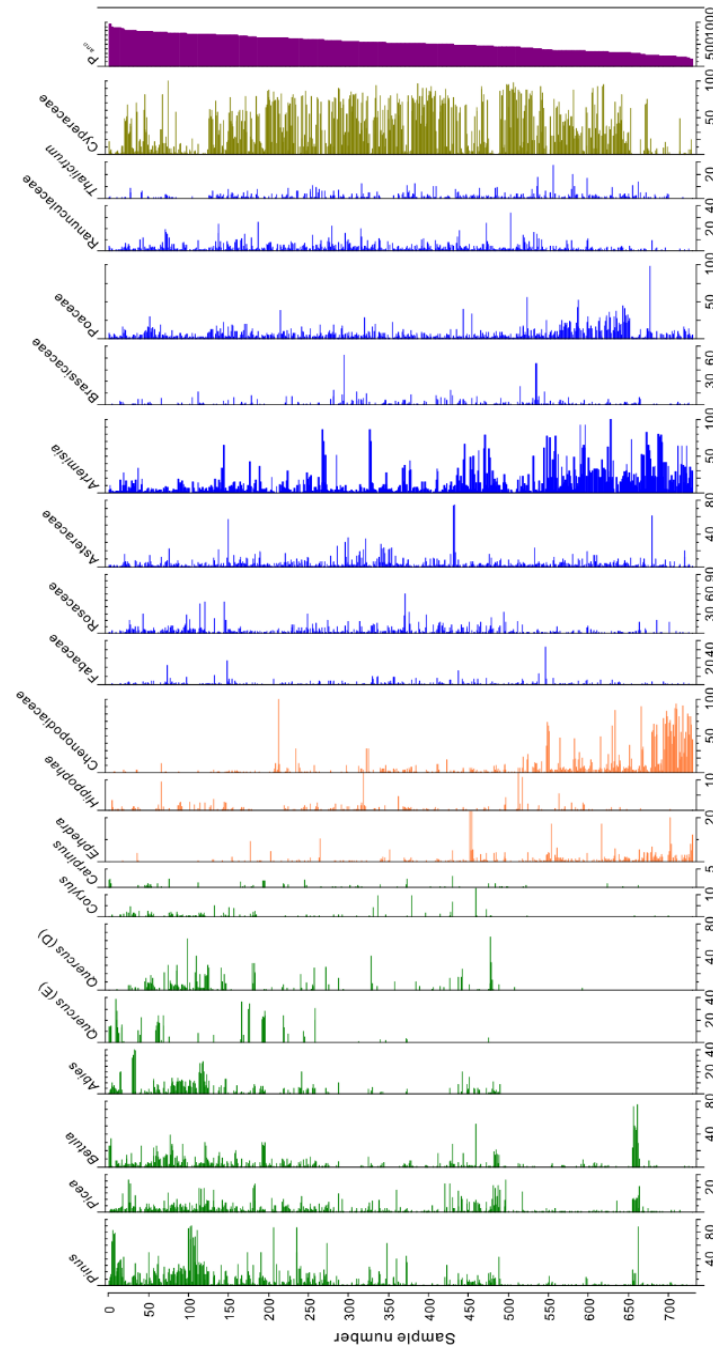


Figure 2. Pollen assemblages of surface sediment samples with annual precipitation (P_{ann}) from the eastern Tibetan Plateau.

450 mm and Mt_{co} lower than $-15^{\circ}C$, although their high abundances are restricted to warm and wet areas (Fig. 2; A1). Drought-tolerant *speciestaxa* such as Chenopodiaceae and *Ephedra* are restricted to regions with low P_{ann} and high Mt_{wa} , and they have quite low abundances in wet areas (Fig. 2-2). In addition, elevation is also an important factor influencing the pollen distribution on the eastern Tibetan

Plateau. Arboreal pollen taxa including *Pinus*, *Picea*, *Abies*, *Betula*, *Quercus* (deciduous, D), and *Corylus* are mainly distributed in areas below 3900 m a.s.l., while *Quercus* (E) is concentrated in areas above 3700 m a.s.l. The high percentages of *Cyperaceae*, *Artemisia*, and *Chenopodiaceae* are mainly concentrated in the lower elevations (below 3200 m a.s.l.).

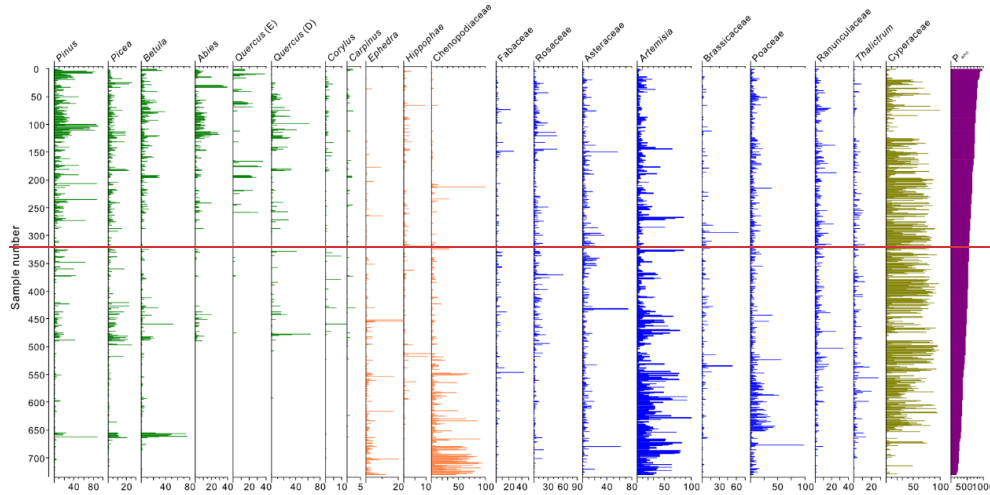


Figure 2. Pollen assemblages of surface sediment samples with annual precipitation (P_{ann}) from the eastern Tibetan Plateau.

Redundancy analysis shows that the first two axes explain 28% of the pollen data (axis 1: 15.5%; axis 2: 12.5%; Fig. 3). Arboreal pollen taxa are located in the left of the biplot and are positively correlated with P_{ann} and Mt_{co} . Asteraceae, Poaceae, *Thalictrum*, Ranunculaceae, Caryophyllaceae, and Cyperaceae show a negative relationship with Mt_{wa} and Mt_{co} while positive with $Elev_7$ and are situated in the lower right of the biplot. Drought-tolerant pollen including Chenopodiaceae, *Artemisia*, and *Ephedra* are situated at the upper right of the biplot, showing positive correlations with temperature variables and negative correlations with precipitation (Fig. 3).

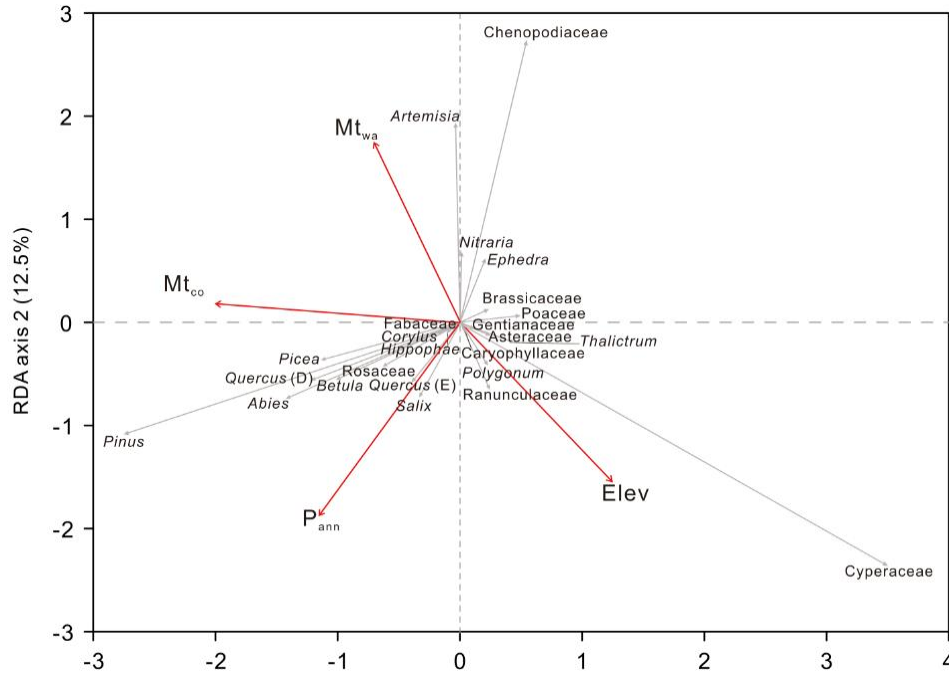


Figure 3. Redundancy analysis (RDA) of modern pollen samples along with three climate variables and elevation.

4.2 Sedimentary lithology and chronology

The sedimentary lithology of the GAH core is comprised of black silt in the upper part (0–99 cm), brown clay in the central part (99–240 cm), and dark-brown fine silt in the lower part (240–329 cm; Fig. 4). Our study concentrates on the vegetation and environment evolution of the upper 176 cm due to the extremely low pollen concentrations in the lower part, insufficient for statistical analyses.

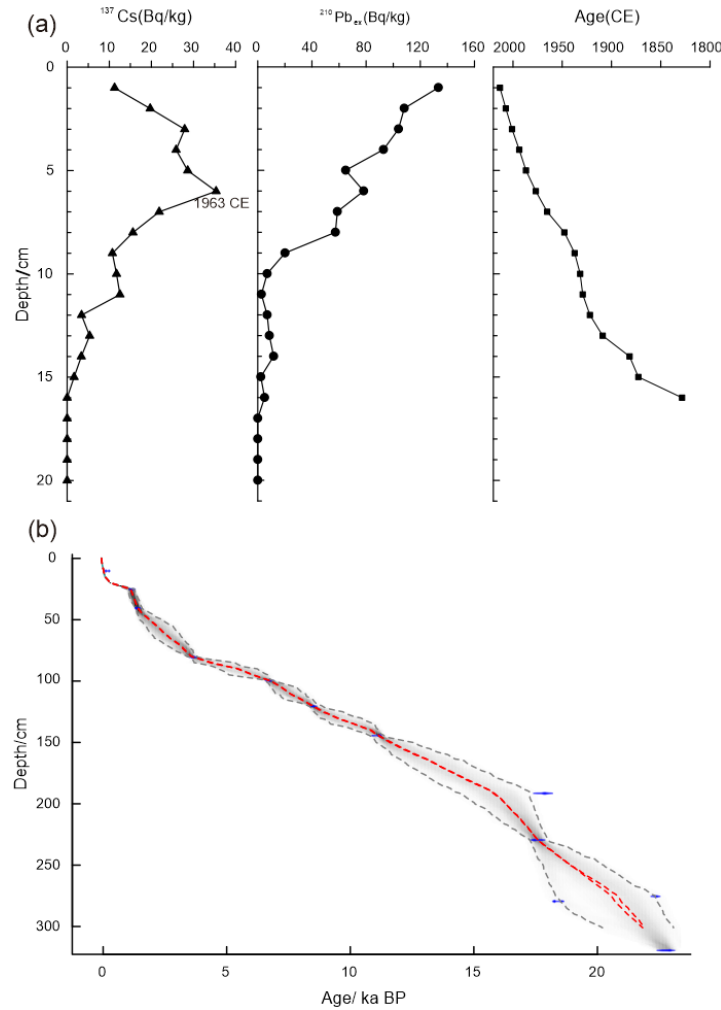


Figure 4. Age-depth model of the Gahai Lake sediment core derived from ^{137}Cs , ^{210}Pb , and ^{14}C dating. (a) Black line with triangles: ^{137}Cs age; black line with solid circles: ^{210}Pb : $^{210}\text{Pb}_{\text{ex}}$ age; black line with squares: mean age based on annual lamination counting. (b) Age-depth curve based on a ^{210}Pb profile of recent sediments and 13 AMS radiocarbon dates from Gahai Lake. The range of the two grey dashed lines indicate the 95% confidence intervals, and the red dashed lines show the single “best” model based on the weighted mean age for each depth.

The chronology of the upper 20 cm sediment is established by the ^{210}Pb -CRS model, with dates falling between 1828 and 2013 CE. The AMS ^{14}C ages of GAH exhibit a linear regression with depth, and the while there is a transient inversion between 191 and 279 cm, which is probably due to increased erosion input to the basin, leading to some old carbon accumulating in the lake. The ages of the upper 20 cm are calculated based on their relationship (Table 2). The), and the age difference between ^{14}C and

²¹⁰Pb of the same depth is considered as the reservoir age. We selected two depths (6 cm and 10 cm) to calculate an average to reduce errors and obtained a reservoir age of 483 years. The age-depth model suggests that the basal age of GAH is about 24 ka BP, and the sedimentation rate is relatively stable (Fig. with the age of sediments between 191 and 279 cm basically remaining the same, probably because of lake sediment collapse or rapid input of terrigenous clastic materials since the lithology also changes markedly between 190 and 280 cm, confirming that the lake underwent rapid deposition during this phase. The sedimentation rate is relatively stable since 15 ka BP, and our research focuses on the vegetation and environmental evolution since 14.2 ka BP (Fig. 4).

Table 2. AMS radiocarbon dates for Gahai Lake

Lab ID	Depth (cm)	$\delta^{13}\text{C}$ (‰)	^{14}C age (yr BP)	Error (\pm yr)
Beta-546102	10	-25.6	440	30
Beta-546103	25	-25.1	1740	30
Beta-539751	40	-25.7	1960	30
Beta-539752	80	-24.8	3880	30
Beta-546104	99	-24.3	6390	30
Beta-539753	120	-22.1	8180	40
Beta-546105	144	-22.9	10240	30
<u>Beta-539754</u>	<u>170</u>	<u>-23</u>	<u>10590</u>	<u>30</u>
Beta-575823	191	-24.4	15070	40
Beta-546120	229	-25.4	14870	50
Beta-550230	275	-23.5	18930	60
Beta-546121	279	-22.6	15550	50
Beta-546122	319	-20.5	19440	70

4.3 Pollen record of GAH since the last deglacial

In our study, 52 pollen taxa were identified in the 111 samples from the upper part of GAH (0–176 cm), with Cyperaceae, *Pinus*, Asteraceae, and *Artemisia* as dominant taxa, while Poaceae, Ranunculaceae, *Ulmus*, and *Picea* are common taxa. The pollen record can be demarcated into four zones (Fig. 5). Pollen concertation is extremely

low (mean 33.5 grains/g) before 7.4 ka BP, and the pollen spectra are dominated by

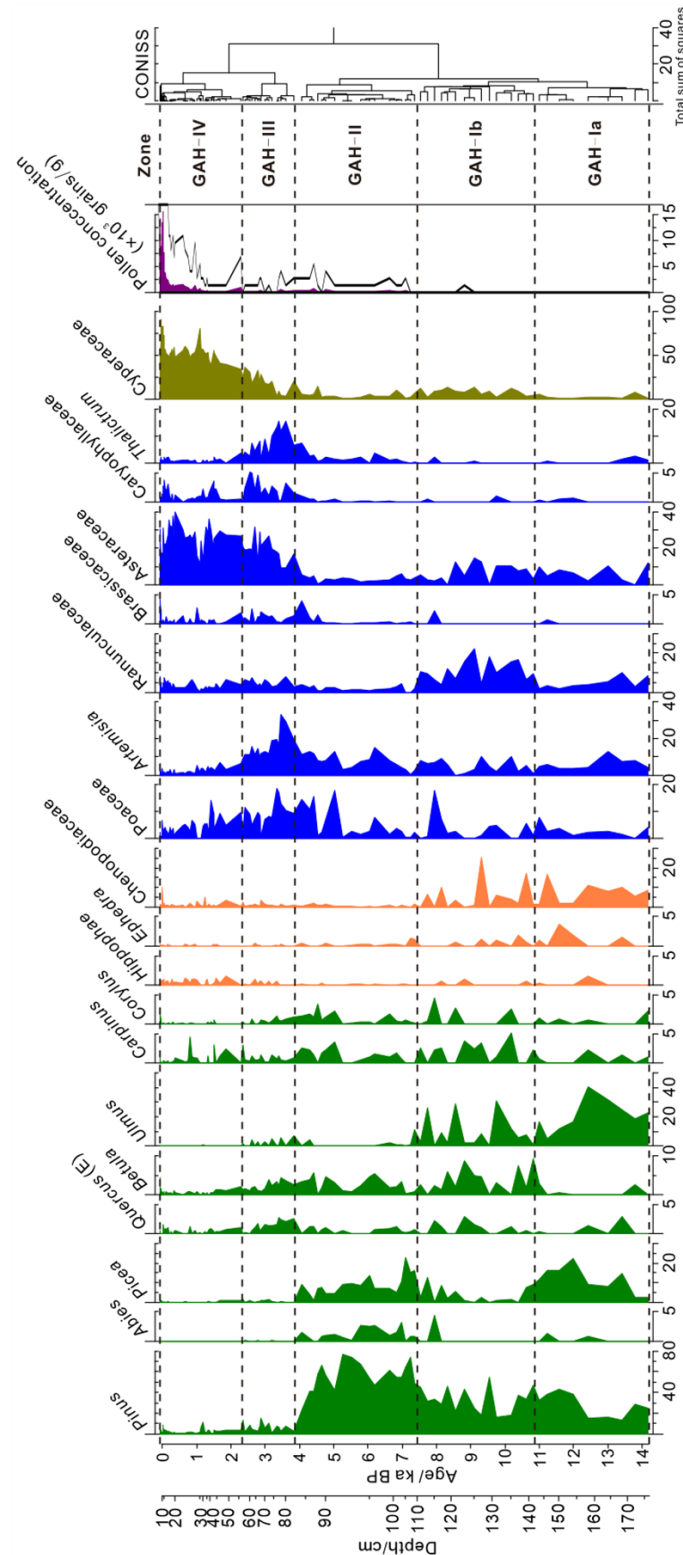
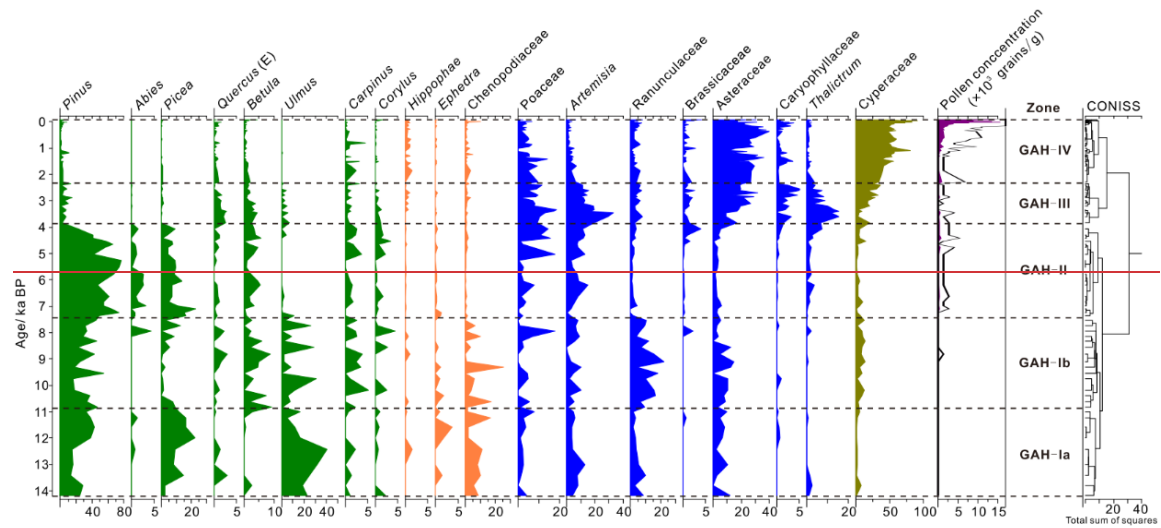


Figure 5. Pollen diagram of the main fossil pollen taxa in Gahai Lake, north-east Tibetan Plateau.

arboreal pollen taxa including *Pinus*, *Picea*, *Ulmus*, and *Betula*, together with abundant drought-tolerant pollen taxa (such as *Chenopodiaceae* and *Ephedra*). Pollen

~~concentration~~ increases remarkably after 7.4 ka BP, and ~~the percentage of~~
drought-tolerant pollen taxa ~~decreased~~ while ~~that of~~ *Pinus* increases in the
pollen spectra. Between 7.43.8 and 2.3 ka BP, *Pinus* and *Picea* decrease sharply,
while *Artemisia*, Poaceae, Asteraceae, and *Thalictrum* increase significantly. Pollen
~~concentration~~ increases greatly and the pollen spectra are dominated by
Cyperaceae after 2.3 ka BP. Cyperaceae rises sharply and becomes overwhelmingly
dominant in the pollen spectra, and the pollen concentration also increases strongly in
the last 0.24 ka BP (Fig. 5).



~~Figure 5. Pollen diagram of the main fossil pollen taxa in Gahai Lake, north-east Tibetan Plateau.~~

4.4 PCA results

The first two axes of the principal component analysis (PCA) explain 72% of the total
pollen data (axis 1: 59.2%; axis 2: 12.8%; Fig. 6a). The PCA divides arboreal pollen
taxa (such as *Pinus*, *Picea*, *Betula*, *Ulmus*), alpine steppe taxa (including *Artemisia*,
Poaceae, Asteraceae), and meadow taxa (Cyperaceae) into three clear groups. In
addition, pollen samples of Zones I and II are consistent with arboreal taxa, pollen
samples from Zone III contain abundant steppe taxa, while samples in Zone IV are
dominated by Cyperaceae (Fig. 6b).

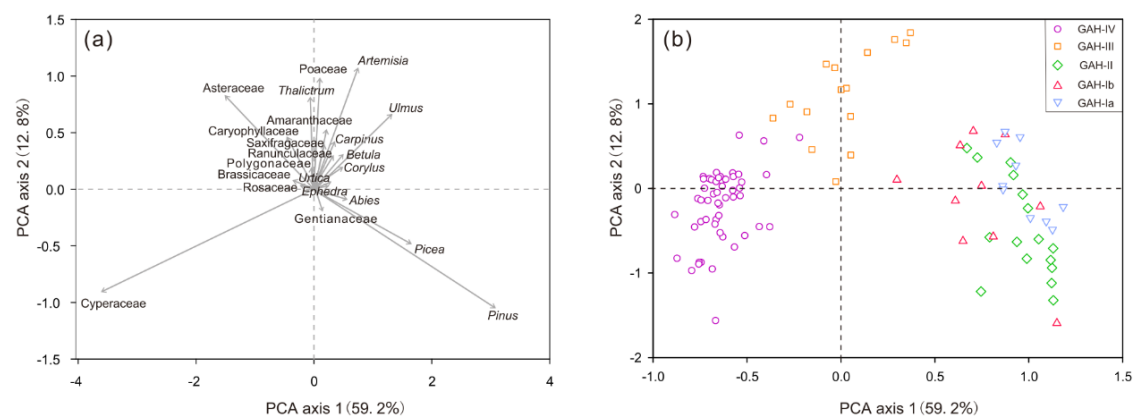


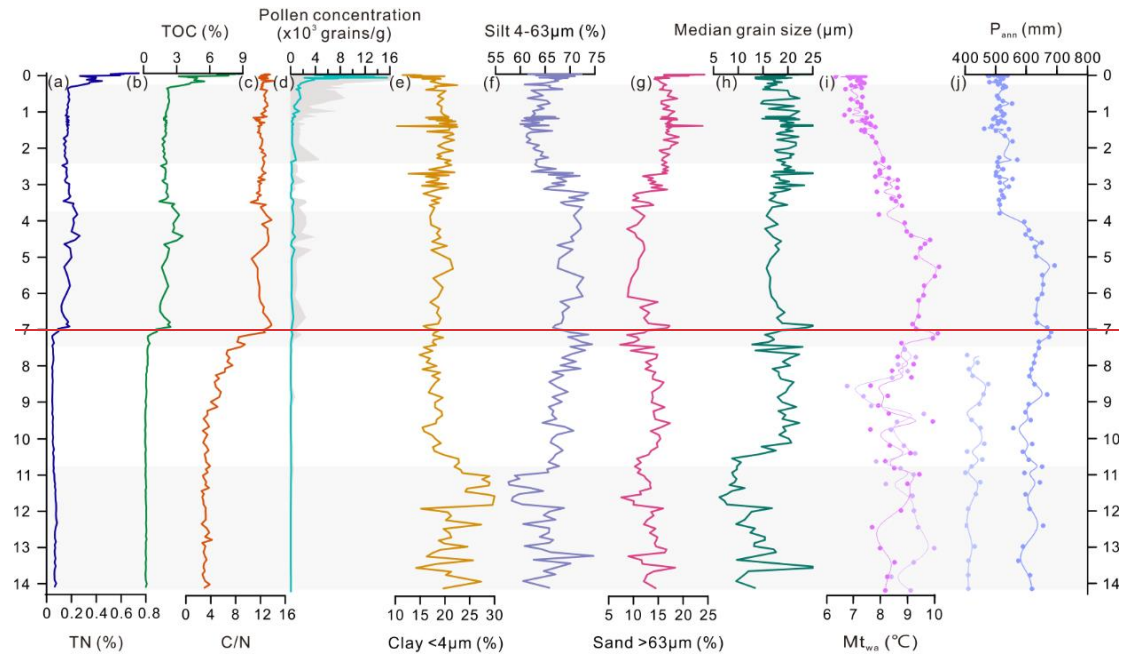
Figure 6. Principal component analysis (PCA) of fossil pollen taxa (a) and pollen zones (b) from Gahai Lake (see Fig. 5 for the pollen zones).

4.5 Sedimentology and conventional geochemistry

The size fractions (volume, %) were classified as clay (<4 μm), silt (fine: 4–16 μm ; medium: 16–32 μm ; coarse: 32–63 μm – combined into one category for the discussion), and sand (>63 μm), and the specific details are shown in Fig. A2. The grain-size ~~resultsparameters~~ of GAH ~~suggest an increasing trend generally include~~ mean grain size, which ~~could be divided into four stages, with theranges~~ from 17.5 to 60 μm . The combined silt fraction (4–63 μm) ~~accountingaccounts~~ for the maximal proportion (58–75%; mean 66%) in general (Fig. 7). The clay fraction (<4 μm ; (15–33%; mean 23%) forms the highest proportion during 14.2–10.8 ka BP, then decreases significantly and remains stable after 10.8 ka BP (Fig. 7). The silt fraction (57.6–74.7%; mean 63.9%) is lowest during 14.2–10.8 ka BP, then increases and reaches a peak during 7.4–3.8 ka BP, after which the mean value decreases to 65.8% (Fig. 7). The sand fraction correlates with the silt fraction before 10.8 ka BP, while median grain size is very low. The silt fraction increases while the clay fraction decreases during 10.8–3.8 ka BP, and the sand fraction (>63 μm) and median grain size first increase and then decrease. The sand fraction and median later the variation is anticorrelated. Mean grain size slightly increase while the clay fraction tends to decrease after 3.8 ka BP, and the silt fraction increases first and then decreases.closely correlates with the sand fraction in general (Fig. 7).

TOC, TN, and C/N ratios fluctuate greatly ~~sinceafter~~ 14.2 ka BP, and TOC and TN

present simultaneous change trends (Fig. 7). TOC and TN values are remarkably low and C/N ratios are lower than 10 between 14.2 and 7 ka BP. TOC, TN, and C/N ratios increase significantly and C/N ratios are higher than 10 between 7 and 43.8 ka BP. TOC, TN, and C/N ratios reduce slightly but are still higher than 10 after 43.8 ka BP. TOC and TN values increase drastically while C/N ratios have no obvious change during the last 0.24 ka BP (since 1710 CE).



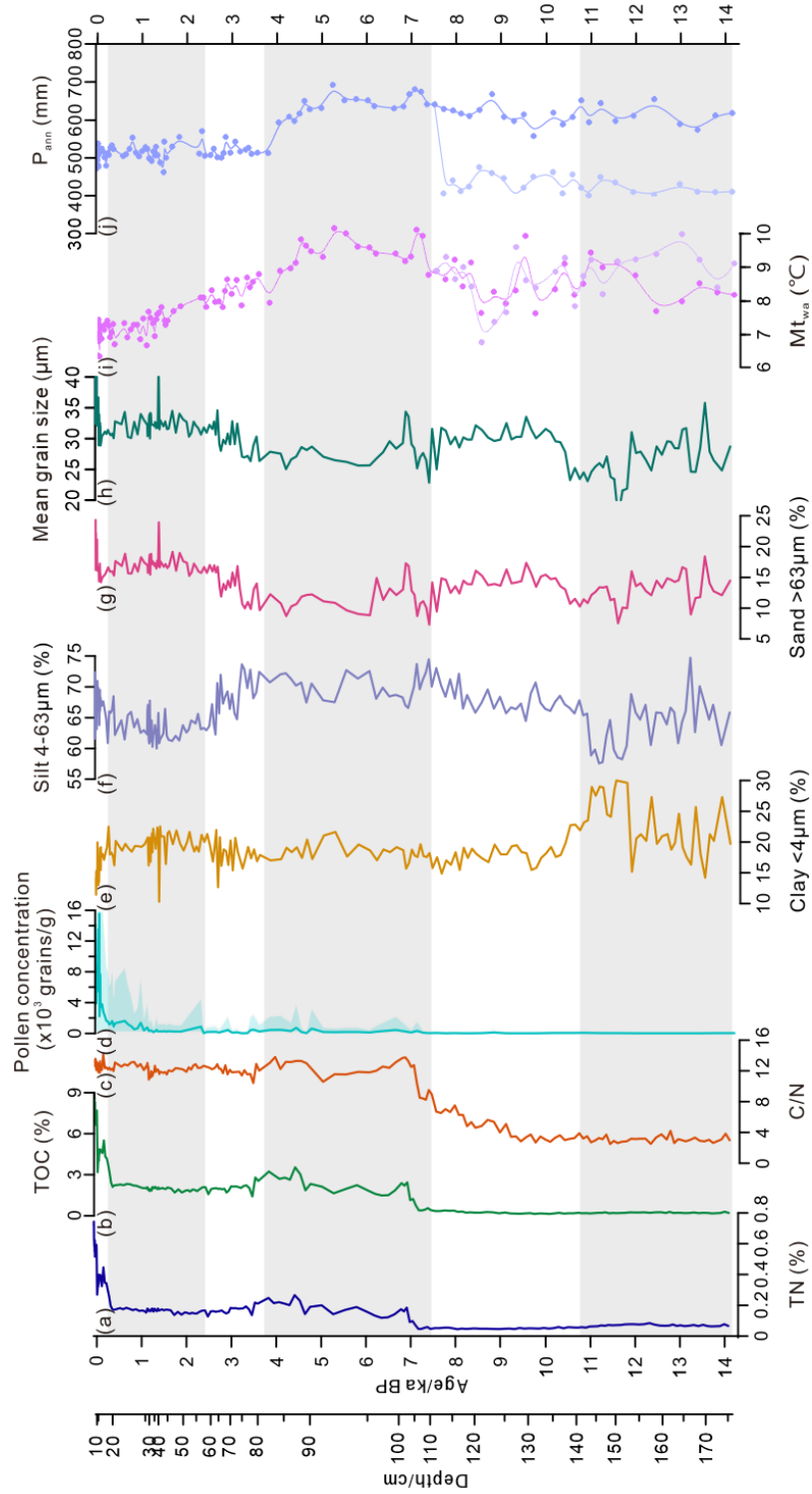


Figure 7. Comparison of the multi-proxy records from Gahai Lake. (a) Total nitrogen (TN); (b) total organic carbon (TOC); (c) C/N ratio; (d) pollen concentration; (e-h) grain size distribution and median mean grain size; (i) quantitative reconstruction of mean temperature of the warmest month (Mt_{wa}). Purple curve indicates the reconstruction based on the pollen assemblages including the arboreal pollen and the light purple curve represents the reconstruction based on the

pollen assemblages removing the arboreal pollen (before 7.4 ka only); (j) the quantitative reconstruction of mean annual precipitation (P_{ann}) and mean temperature of the warmest month (Mt_{wa}). The dark curves are the reconstructions based on the pollen assemblages including the arboreal pollen, and the light blue curves are the reconstructions based on the pollen assemblages without the arboreal pollen (before 7.4 ka only). The grey shading denotes the different pollen zones of Gahai Lake.

5 Discussion

5.1 Patterns and interpretation of the proxies

TOC is a proxy for the abundance of organic matter which originates from aquatic organisms and terrestrial vegetation, and TN represents the nutritional conditions of the lake. In addition, TOC is an effective index to evaluate the summer monsoon intensity, where low values reflect a cold and dry climate (An et al., 2012; Optiz et al., 2012). C/N ratios are used to trace the plant source of the organic matter. C/N ratios of the nonvascular aquatic plants and algae are generally between 4 and 10, and C/N ratios >20 indicate that organic matter mainly originates from terrestrial vascular plants. Ratios ranging from 10 to 20 suggest that the organic matter is derived from a mixture of aquatic and terrestrial plants (Meyers and Ishiwatari, 1993; Meyers, 2003; Kasper et al., 2015). High values of TOC and C/N ratios in the Tibetan Plateau lakes suggest a warm and wet climate (Chen et al., 2021).

The grain-size composition of lake sediments can be used to trace the source of clastic particles, aeolian activity, and water-level fluctuations, which reflect the regional climate conditions (Håkanson and Jansson, 1983; Liu et al., 2016). The sources of lacustrine sediments include clastic materials carried by inflow rivers, aeolian inputs, and authigenic chemical deposition, and mean grain size reflects the intensity of transport dynamics (Folk and Ward, 1957; Xiao et al., 2013). There have been many particle-size analyses from lacustrine sediments and modern surface sediments suggest or loess deposits on the north-eastern Tibetan Plateau. For example, Qiang et al. (2014) analysed the grain size of Genggahai lake and propound that the sand

fraction ($>63\ \mu\text{m}$) ~~or particles $>50\ \mu\text{m}$ are mainly transported by wind and could be an indicator of reflects~~ aeolian activity ~~(Qiang et al., 2014; Wang et al., 2015; Liu et al., 2016). Particle-size variation can reflect~~. Chen et al. (2013) investigated Sugan Lake in the Qaidam basin and argue that ~~changes in water level, with coarser grains indicating a rise in water level as river discharge would need to be greater to transport the heavier grains, and hence suggesting an increase in precipitation (Håkanson and Jansson, 1983; the $>63\ \mu\text{m}$ Liu et al., 2008)~~. Therefore, we speculate that a high silt fraction ($4-63\ \mu\text{m}$) in Gahai Lake reflects an increase in the lake water level, while a high clay fraction ($<4\ \mu\text{m}$) content reflects a low stand ~~reflect the frequencies of dust storms and strong winds~~. In addition, Wang et al. (2015) analysed a loess deposit from Ledu on the north-eastern Tibetan Plateau and also conclude that a grain-size of $60\ \mu\text{m}$ is locally transported by strong winds during cold climatic intervals. The sand fraction ($>63\ \mu\text{m}$) is also found in modern river sediments although the percentage is typically low. A single extreme rain event under an arid climate could lead to an abrupt sand fraction increase (Ding et al., 2005; Li et al., 2012; Liu et al., 2016; Ota et al., 2017; Zhou et al., 2018). Therefore, the sand fraction is mainly transported by winds and any peak or abnormal increase of the coarse grain size (especially the sand fraction) is likely related to flood events. In our study, a high proportion of the sand fraction ($>63\ \mu\text{m}$) ~~indicates~~ mainly represents aeolian activity intensity. ~~The variation of the median grain size is consistent with the sand fraction thus also reflecting aeolian deposition.~~

Particle-size variation can reflect changes in water level or precipitation, taking into account the different lake recharge types, hydrological conditions, and lake sizes. There has been debate about how to interpret the grain-size index because the coarse particle fraction is positively correlated with precipitation and water level in small lakes dominated by summer rainfall but not in large lakes (Peng et al., 2005; Chen et al., 2021). Gahai Lake is a small, shallow lake and receives most of its precipitation in summer. The coarse particle fraction reflects a humid climate and high lake level owing to strong hydrological dynamics (Håkanson and Jansson, 1983; Peng et al.,

2005; Liu et al., 2008). The silt fraction (4–63 μm) in our study is driven by the medium silt (16–32 μm) fraction, while the fine and coarse silt fractions remain almost unchanged during the Holocene, hence the fine, medium, and coarse silt are combined into the total silt fraction (4–63 μm) for discussion. In addition, the mean grain size is closely related to the sand fraction and poorly reflects the climatic moisture and lake level. Therefore, we speculate that a high silt fraction (4–63 μm) in Gahai Lake reflects an increased lake level, while a high clay fraction ($<4 \mu\text{m}$) content reflects a low stand.

5.2 Determination of exogenous pollen grains

According to modern pollen research from the Tibetan Plateau and northern China, *Pinus*, *Picea*, and *Betula* are dominant pollen taxa in forest samples, and these taxa have a good diffusion capacity ~~and are with their pollen~~ easily transported for long distances from their ~~pollen~~-source (Lu et al. 2004; Ma et al., 2008; ~~Ma et al., 2015~~). *Ulmus* also has a good diffusion and can spread up to 40 km away, and can therefore ~~be~~ show up as a regional vegetation component in a pollen assemblage (Xu et al., 2007). ~~The~~ In addition, we analysed the non-woodland topsoil samples within 30 km of Gahai Lake ($n=22$). Results show that arboreal pollen taxa including *Pinus*, *Picea*, and *Betula* are always present (usually at $<40\%$) in the pollen samples, indicating that they have good diffusivity and are easily transported to areas beyond their pollen source (Fig. A3; A4). Therefore, the main arboreal pollen taxa in the GAH core ~~are thus including~~ *Pinus*, *Picea*, *Betula*, and *Ulmus* are highly diffusive species which may bias the ~~interpretation of the source of arboreal pollen~~ vegetation reconstruction unless their far-distance transport is accounted for.

The main pollen taxa have notable spatial distribution characteristics owing to their ecological environment based on modern pollen research and the modern pollen dataset. Arboreal taxa including *Pinus*, *Picea*, and *Betula* are mainly distributed in a warm and humid environment (Lu et al., 2004). *Ulmus* is a drought-tolerant and light-demanding plant which can survive at precipitation levels lower than 200 mm per year

(Shen et al., 2005). Previous modern pollen studies reveal that Chenopodiaceae and *Ephedra* are commonly found in the desert, indicating a tolerance for dry climatic conditions (Yu et al., 2001; Huang et al., 2018; Qin ~~et al.~~, 2021); and our modern pollen dataset for the east Tibetan Plateau suggests that xerophilous taxa such as *Ephedra* and Chenopodiaceae are restricted to areas with P_{ann} lower than 400 mm, and almost absent in samples with high precipitation (Fig. 2). Fossil pollen spectra from the Tibetan Plateau with abundant arboreal pollen taxa together with low pollen concentrations are considered to represent extreme arid conditions and sparse vegetation (Kramer et al., ~~2010b~~2010; Ma et al., 2019). Therefore, we argue that the arboreal pollen including *Pinus*, *Picea*, and *Ulmus* has been transported by wind from beyond the watershed, and that the high abundance of drought-tolerant herbaceous taxa (weak dispersal ability) and low pollen concentrations indicate a sparse vegetation cover around the lake between 14.2 and 7.4 ka BP, suggesting an extremely arid climate.

5.3 Evolution of vegetation and climate history since the last glacial

Palaeo-vegetation and palaeo-climate is reconstructed based on the fossil pollen, TOC, TN, C/N ratios, and grain-size record of Gahai Lake since the last deglacial.

From 14.2 to 10.8 ka BP, alpine steppe or desert covered the study area with the arboreal pollen derived from the surrounding mountains in the south-east of the basin.

Pollen-based past P_{ann} reconstructions are ~~likely to be overestimated since~~ mainly in the exogenous range of higher than 418 mm (excluding arboreal pollen has not been excluded taxa from the pollen spectra) but less than 610 mm (including arboreal taxa from pollen spectra). Remarkably, however, there is little difference between the reconstructed Mt_{wa} shows no bias from these exogenous based on excluding arboreal taxa (mean 9.1°C) and including arboreal pollen, (mean 9.6°C), thus the climate was probably mild warm and arid during this period (Fig. 7). Quite low TOC and TN contents, and C/N ratios ~~below four~~ (< 4) suggest that the organic matter is mainly derived from aquatic plants, and ~~also imply low~~ little terrestrial biomass productivity

under a dry and cold environment (Fig. 7; Zhu et al., 2015). ~~Clay~~Maximum clay fraction ~~reaches its maximum value, reflecting a~~ and high sand fraction in the lake sediments reflect low water level and ~~weak~~intense aeolian activity (Fig. 7). In summary, Gahai was probably a small and shallow pond ~~under a mild, arid climate~~ during this period, with the surrounding vegetation dominated by alpine steppe or desert.

From 10.8 to 7.4 ka BP, Ranunculaceae and Cyperaceae show a slight increase, and alpine steppe occurs across the region (Fig. 5). The reconstruction suggests that Mt_{wa} (mean: 8.5 to 9.0°C) slightly decreases compared with the former stage, whereas reconstructed P_{ann} (mean: 468 to 619 mm) is basically steady but still ~~reflects~~influenced by the exaggerated contribution of exogenous arboreal pollen (Fig. 7). TOC and C/N ratios rise during the early Holocene, implying an increase in biological productivity although still mainly from aquatic plants (Fig. 7). The silt ~~and sand fractions and median grain size fraction~~ significantly ~~increase,~~increases while the clay fraction decreases sharply with small fluctuations in the sand fraction, indicating ~~that a slight rise in~~ the water level ~~rose~~ and ~~that~~intense aeolian activity ~~strengthened~~ during the early Holocene (Fig. 7). Therefore, we infer that the vegetation of Gahai Basin ~~had a cold and arid climate with enhanced wind strength~~ was covered by alpine steppe under dry climatic conditions during the early Holocene, ~~and an alpine steppe vegetation while the lake had an increased water level.~~

~~The pollen concentration, silt fraction, TOC, and TN remarkably increase, and C/N ratios above 10 suggest that the climate and vegetation greatly improved after 7.4 ka BP to reach an optimum. Gahai Lake was at a high stand with increased terrestrial organic matter input (Fig. 7). We infer that Gahai Lake grew from a small pond and that the pollen spectra mainly reflect vegetation change within the catchment, with the reconstructed P_{ann} and Mt_{wa} reflecting the regional climate variation with weak influence from exogenous pollen during the mid-Holocene (Fig. 7).~~ The pollen spectra are dominated by *Pinus* and *Picea* while drought-tolerant taxa (such as *Chenopodiaceae* and *Ephedra*) have ~~a low~~ ~~abundance~~abundances, indicating a

vegetation shift from alpine steppe to montane forest between 7.4 and 3.8 ka BP (~~Ma et al., 2008; Zhao et al., 2009~~). In addition, the pollen concentration increases markedly, reflecting a greatly enhanced vegetation and better climate after 7.4 ka BP (Kramer et al., 2010; Ma et al., 2019). The climate reconstruction shows that P_{ann} (mean: 634 mm) and Mt_{wa} (mean: 9.3 °C) reach their peaks, suggesting that Gahai Lake is under a warm and wet climate (P_{ann} and Mt_{wa} reach their peaks; Fig. 7). In addition, the optimum during this period (Fig. 7). In addition, the silt fraction significantly increases to a peak (mean: 70%), and TOC, TN, and C/N ratios (> 10) markedly increase suggesting that Gahai Lake was at a high stand with increased terrestrial organic matter input having grown from a small pond since 7.4 ka BP. At the same time, the sand fraction and median grain size slightly decline suggesting weaker decreases to its nadir (mean: 11.7%), indicating weakened aeolian activity during this period (Fig. 7, which could be related to the increased vegetation cover and moisture (Fig. 7). In summary, as Gahai Lake expanded, the surrounding vegetation became montane forest as seen by a shift in the arboreal pollen from extra-regional to within catchment. To support this vegetation, the climate was warm and wet, while aeolian activity was weak during the mid-Holocene (Fig. 7).

During Between 3.8 to and 2.3 ka BP, the pollen spectra are characterised by a high percentage of Poaceae, *Artemisia*, and Asteraceae (major component components of alpine steppe), and while arboreal pollen taxa, especially *Pinus* and *Picea*, sharply decrease, indicating the tree-line retreated to a lower elevation and a shift in vegetation type to alpine steppe (Herzschuh et al., 2010; Shen et al., 2021; Fig. 5). Reconstructed P_{ann} (mean: 547 mm) and Mt_{wa} (mean: 8.3 °C) decrease significantly, suggesting mild and arid climatic conditions deteriorated (Fig. 7). TOC, TN, and C/N ratios slightly decrease compared with the previous stage, suggesting the weakened input of organic matter although the source remains unchanged weakened (Fig. 7). The silt fraction substantially decreases while the sand fraction and median grain size have has an increasing trend, suggesting weaker hydrodynamic conditions and strengthened the lake level decreased and aeolian activity increased (Fig. 7). In brief,

the climate ~~turned mild and~~tended to be arid ~~and with enhanced~~ aeolian activity ~~strengthened and deteriorating environmental conditions~~. Alpine steppe dominated across the study region during this period.

From 2.3 to 0.24 ka BP, the dominant taxa change from alpine steppe (Poaceae, *Artemisia*, and Asteraceae) ~~components~~ (Ma et al., ~~2015~~2017; Qin ~~et al.~~et al., 2021) to alpine meadow (Cyperaceae) components (Herzschuh et al., 2007; 2010; Fig. 5), and a decrease in reconstructed P_{ann} (537 mm) and Mt_{wa} reconstruction reveals a (-7.3 °C) suggests an arid and cold environment (Fig. 7). TOC, TN, and C/N ratios ~~suggest~~ ~~there are almost unchanged suggesting similar~~ total biogenic productivity ~~input and its~~ ~~source has little changed compared with the~~ to the previous stage (Fig. 7). ~~Silt~~The silt fraction decreases while the sand fraction ~~and median grain size increase~~increases, indicating ~~weaker water dynamics~~ a lower lake level and ~~enhanced~~stronger aeolian activity than the former stage. Therefore, in this period, the vegetation turned to alpine meadow under an arid and cold climate, and lake level dropped while aeolian activity increased.

After 0.24 ka BP (1710 CE), the pollen spectra are dominated by Cyperaceae (maximum, 95%; Fig. ~~5~~5), with the percentage of Poaceae decreasing while Ranunculaceae increases. Previous vegetation investigations suggest that overgrazing causes the proportion of Cyperaceae to increase and become the dominant taxon, and thus could be an indicator of human activities (Yuan et al., ~~2004~~2004; ~~Dong et al.~~2004; ~~Miehe et al.~~2014; ~~Lin et al.~~2016); 2004; Miehe et al., 2014; Lin et al., 2016). In addition, modern pollen research also suggests that pollen assemblages are dominated by Cyperaceae in overgrazed sites of alpine steppe and alpine meadow (Duan et al., 2021). According to earlier topsoil studies, Ranunculaceae and Poaceae are important indicators of grazing activities on the north-east Tibetan Plateau, with pollen percentages changing significantly in the overgrazed sites (Wei et al., 2018; Duan et al., 2021). Hence the vegetation during this period could have been disturbed by human activities. In addition, TOC, TN, and pollen concentration notably increase, indicating terrestrial material input strengthened, possibly as a result of increased

surface erosion (silt fraction increases; Fig. 7) due to the destruction of vegetation by ~~human activities~~grazing and pastoral activities. Reduced precipitation and monsoonal activity are also suggested by the increases in TOC, TN, and pollen concentration.

5.4 Comparison of the regional climate and vegetation records from the north-east Tibetan Plateau in the early Holocene

Climate and vegetation as revealed by pollen records covering the early Holocene on the north-east Tibetan Plateau are inconsistent, which may be due to the following reasons: local factors have a greater effect than regional climate (Chen et al., 2020); the distance of sampling sites from forested areas affects the results of vegetation reconstruction (Sun et al., 2017); and different climatic factors influence the regional vegetation distribution of the eastern Tibetan Plateau (Zhao et al., 2011). Based on the results of TOC, ~~TN~~, grain size, and reconstructed precipitation based on pollen analysis, we infer that Gahai Lake was surrounded by alpine steppe vegetation under ~~cool and an~~ arid ~~climatic conditions~~climate, and that the arboreal pollen was mainly transported by wind from the surrounding mountains during the early Holocene. (Fig. 8a; b; c). Other records from the north-east Tibetan Plateau ~~confirm~~support these general features of climate and vegetation during the early Holocene. For example, ~~results~~reconstructions from ~~an~~-adjacent ~~peatland areas~~ show that the climate and vegetation of the Zoige Basin and ~~Nianbaoyeze Mountains~~Ximencuo Lake based on the pollen records reached their optimum during the mid-Holocene and had a cooler temperature and lower humidity during the early Holocene (Fig. 8f, g, h, i; Zhou et al., 2010; Zhao et al., 2011; Sun et al., 2017; Herzschuh et al., 2014). ~~A reconstruction~~ Multi-proxies (e.g. carbonate content, oxygen and carbon stable isotope compositions of authicarbonate) also from ~~Hurleg~~Gahai Lake ~~also indicate~~suggest that ~~the~~ climate was ~~at a low standard~~arid, becoming warm during the early Holocene and ~~that the vegetation type was desert or desert steppe~~ (~~Zhao~~then moist, on the whole, during the mid-Holocene (Chen et al., 2007; ~~Fan et al., 2014~~).). Cheng et al. (2009) ~~analyse~~(2013) analysed the pollen record of Dalianhai Lake (from 16 ka BP) and

conclude that this region had a dry climate and was covered by steppe desert during the early Holocene (Fig. 8d). Multi-proxy records from Qinghai Lake including pollen, carbonate, TOC, TN, $\delta^{13}\text{C}$ of organic matter (Shen et al., 2005), redness records (Ji et al., 2005), and

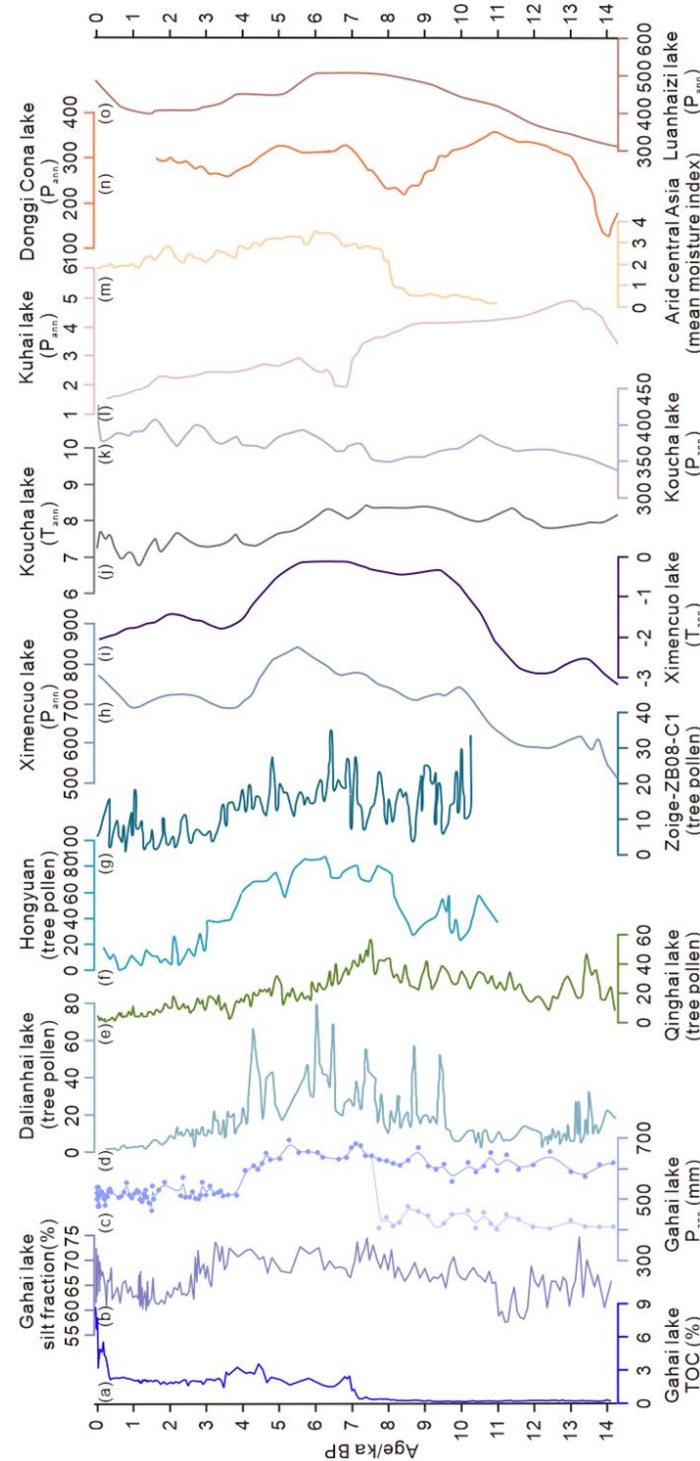


Figure 8. Comparison of the Gahai Lake results with other lake level (Liu et al., 2015) records on the north-eastern Tibetan Plateau. (a-c) Total organic carbon (TOC), silt fraction, and pollen-

based precipitation reconstruction of the Gahai Lake record (this paper); (d) arboreal pollen percentages of Dalianhai Lake (Cheng et al., 2013); (e) arboreal pollen percentages of Qinghai Lake (Shen et al., 2005); (f) arboreal pollen percentages of the Hongyuan peatland (Zhou et al., 2010); (g) arboreal pollen percentages of the central Zoige basin (Zhao et al., 2011); (h-i) P_{ann} and T_{ann} reconstructed from pollen records from Ximencuo Lake (Herzschuh et al., 2014); (j-k) T_{ann} and P_{ann} reconstructed from pollen records from Koucha Lake (Herzschuh et al., 2009); (l) P_{ann} reconstructed from pollen records from Kuhai Lake (Wischnewski et al., 2011); (m) synthesized mean moisture index of arid central Asia (Chen et al., 2008); (n) P_{ann} reconstructed from pollen records from Donggi Cona Lake (Wang et al., 2014); (o) P_{ann} reconstructed from pollen records from Donggi Cona Lake (Herzschuh et al., 2010).

lake level reveal that this region had a dry climate and weak East Asian summer monsoon (Fig. 8e; Shen et al., 2005; Ji et al., 2005; Liu et al., 2015; Chen et al., 2016). Similar records are found from Koucha Lake (Fig. 8j, k; P_{ann} and T_{ann} based on pollen record; Herzschuh et al., 2009), Kuhai Lake (Fig. 8l; P_{ann} based on pollen record; Wischnewski et al., 2011), ~~Luanhaizi Lake (Herzschuh et al., 2005; 2010), and the~~ arid region of central Asian (moisture variation based on eleven records integrated during the early Holocene-~~(~~: Fig. 8m; Chen et al., 2008; 2020), and Luanhaizi Lake (Fig. 8o; T_{ann} based on pollen record; Herzschuh et al., 2005; 2010). The pollen assemblages of Donggi Cona Lake show a high percentage of *Ephedra*, which suggests an arid environment in the early Holocene, although the quantitative reconstruction (Fig. 8n; P_{ann} based on pollen record) shows this period ~~was~~ the wettest stage in the Holocene (~~Tian~~Wang et al., 2014; Huang et al., 2018). Based on the above investigations, we can conclude that the climate was arid on the north-east Tibetan Plateau during the early Holocene.

6. Conclusions

Based on modern pollen investigations for the ~~east~~eastern Tibetan Plateau, arboreal pollen can be determined as exogenous taxa when they appear together with drought-

tolerant taxa and low pollen concentrations in fossil pollen spectra. The Gahai Basin was covered by ~~the~~ alpine steppe or desert under ~~a cold and dry~~ climateclimatic conditions during 14.2–7.4 ka BP; montane forest migrated into the basin and the climate reached an optimum between 7.4 and 3.8 ka BP according to the evidence of TN, TOC, C/N, and grain-size records; the vegetation reverted to alpine steppe owing to a drying climate duringfrom 3.8 ~~andto~~ 2.3 ka BP, after which steppe was replaced by alpine meadow as the climate cooled. In addition, the vegetation showed signs of being influenced by human activity during the last 0.24 ka BP.

Data availability. The data used in this study can be obtained from the corresponding author Xianyong Cao (xcao@itpcas.ac.cn).

Author contribution. NW extracted and identified pollen samples, ~~analyzed~~analysed pollen data and wrote manuscript; LL, XH, and YZ participated in sample collecting and data analysis; HW contributed to the detailed comments; XC designed this study and led interpretation. All authors commented and improved manuscript.

Competing interests. The authors declare that they have no conflict of interest.

Acknowledgements. This study was supported by the Basic Science Center for Tibetan Plateau Earth System (BSCTPES, NSFC project No. 41988101), the National Natural Science Foundation of China (Grant No. 41877459) and CAS Pioneer Hundred Talents Program (Xianyong Cao). We thank Cathy Jenks for help with language editing.

References

An, Z., Colman, S. M., Zhou, W., Li, X., Brown, E. T., Jull, A. J. T., Cai, Y., Huang, Y., Lu, X. ~~F.~~, Chang, H., Song, Y. ~~G.~~, Sun, Y. ~~B.~~, Xu, H., Liu, W. ~~G.~~, Jin, Z. ~~D.~~, Liu, X. ~~D.~~, Cheng, P., Liu, Y., Ai, L., Li, X., Liu, X., Yan, L., Shi, Z., Wang, X., Wu, F.,

- Qiang, X.-K., Dong, J., Lu, F., and Xu, X.: Interplay between the westerlies and Asian monsoon recorded in Lake Qinghai sediments since 32 ka. *Sci. Rep.* **2**, 619, <https://doi.org/10.1038/srep00619>, 2012.
- Andersen, K. K., Azuma, N., Barnola, J. M., Bigler, M., Biscaye, P., Caillon, N., Chappellaz, J., Clausen, H. B., DahlJensen, D., Fischer, H., Fluckiger, J., Fritzsche, D., Fujii, Y., Goto-Azuma, K., Gronvold, K., Gundestrup, N. S., Hansson, M., Huber, C., Hvidberg, C. S., Johnsen, S. J., Jonsell, U., Jouzel, J., Kipfstuhl, S., Landais, A., Leuenberger, M., Lorrain, R., Masson-Delmotte, V., Miller, H., Motoyama, H., Narita, H., Popp, T., Rasmussen, S. O., Raynaud, D., Rothlisberger, R., Ruth, U., Samyn, D., Schwander, J., Shoji, H., Siggard-Andersen, M. L., Steffensen, J. P., Stocker, T., Sveinbjornsdottir, A. E., Svensson, A., Takata, M., Tison, J. L., Thorsteinsson, T., Watanabe, O., Wilhelms, F., and White, J. W. C.: High-resolution record of Northern Hemisphere climate extending into the last interglacial period, *Nature*, **431**, 147–151, <https://doi.org/10.1038/nature02805>, 2004.
- Birks, H. J. B.: Contributions of Quaternary botany to modern ecology and biogeography, *Plant Ecol. Diversity* **12**, 189–385, <https://doi.org/10.1080/17550874.2019.1646831>, 2019.
- Blaauw, M., and Christen, J. A.: Flexible paleoclimate age-depth models using an autoregressive gamma process, *Bayesian Anal.*, **6**: 457–474, <https://doi.org/10.1214/ba/1339616472>, 2011.
- Blaauw, M., Christen, J. A., Aquino Lopez, M. A., Esquivel Vazquez, J., Gonzalez V. O. M., Belding, T., Theiler, J., Gough, B., and Karney, C.: rbacon: age-depth modelling using Bayesian statistics, <https://cran.r-project.org/web/packages/rbacon/index.html>. Accessed Jan 2020, 2021.
- Bryson, R. A.: Airstream climatology of Asia. Proceedings of International Symposium on the Qinghai-Xizang Plateau and Mountain Meteorology. American Meteorological Society, Boston, MA, pp. 604–617, 1986.
- Cao, X., Herzschuh, U., Telford, R. J., and Ni, J.: A modern pollen–climate dataset

from China and Mongolia: Assessing its potential for climate reconstruction, *Rev. Palaeobot. Palyno.*, 211, 87–96, <https://doi.org/10.1016/j.revpalbo.2014.08.007>, 2014.

Cao, X., Tian, F., Li, K., and Ni, J.: Atlas of pollen and spores for common plants from the east Tibetan Plateau, National Tibetan Plateau Data Center, <https://doi.org/10.11888/Paleoenv.tpdc.270735>, 2020.

Cao, X., Tian, F., Li, K., Ni, J., Yu, X., Liu, L., and Wang, N.: Lake surface-sediment pollen dataset for the alpine meadow vegetation type from the eastern Tibetan Plateau and its potential in past climate reconstructions, *Earth Syst. Sci. Data*, 13, 3525–3537, <https://doi.org/10.5194/essd-13-3525-2021>, 2021.

Chen, F., Qiang, M., Zhou, A., Xiao, S., Chen, J., and Sun, D.: A 2000-year dust storm record from Lake Sugan in the dust source area of arid China, *J. Geophys. Res.*, 118, 2149–2160, <https://doi.org/10.1002/jgrd.50140>, 2013.

Chen, F., Dong, G., Zhang, D., Liu, X., Jia, X., An, C., Ma, M., Xie, Y., Barton, L., Ren, X., Zhao, Z., Wu, X., and Jones, M. K.: Agriculture facilitated permanent human occupation of the Tibetan Plateau after 3600 B.P., *Science*, 347, 248–250, [doi: 10.1126/science.1259172](https://doi.org/10.1126/science.1259172), 2015.

Chen, F., Wu, D., Chen, J., Zhou, A., Yu, J., Shen, J., Wang, S., and Huang, X.: Holocene moisture and East Asian summer monsoon evolution in the north-eastern Tibetan Plateau recorded by Lake Qinghai and its environs: a review of conflicting

- proxies. *Quat. Sci. Rev.* 154, 111–129,
<https://doi.org/10.1016/j.quascirev.2016.10.021>, 2016.
- Chen, F., Yu, Z., Yang, M., Ito, E., Wang, S., Madsen, D. B., Huang, X., Zhao, Y., Sato, T., Birks, H. J. B., Boomer, I., Chen, J., An, C., and Wünnemann, B.: Holocene moisture evolution in arid central Asia and its out-of-phase relationship with Asian monsoon history. *Quat. Sci. Rev.* 27, 351–364,
<https://doi.org/10.1016/j.quascirev.2007.10.017>, 2008.
- Chen, F., Zhang, J., Liu, J., Cao, X., Hou, J., Zhou, L., Xu, X., Liu, X., Wang, M., Wu, D., Huang, L., Zeng, T., Zhang, S., Huang, W., Zhang, X., and Yang, K.: Climate change, vegetation history, and landscape responses on the Tibetan Plateau during the Holocene: A comprehensive review. *Quat. Sci. Rev.*, 243, 106444,
<https://doi.org/10.1016/j.quascirev.2020.106444>, 2020.
- Chen, H., Zhu, L., Wang, Y., Ju, J., Ma, Q., and Xu, T.: Paleoclimate changes over the past 13,000 years recorded by Chibuzhang Co sediments in the source region of the Yangtze River, China, *Palaeogeogr. Palaeoclimatol. Palaeoecol.*, 573, 110433, <https://doi.org/10.1016/j.palaeo.2021.110433>, 2021.
- Chen, Z., Ma, H., Cao, G., Zhang, X., Zhou, D., Yao, Y., Tan, H., and Gao, Z.: Climate-environmental evolution in Gahai Lake area of Qaidam Basin since Late Last Deglacial Period, *Geochimica*, 36, 578–584, 2007 (in Chinese with English abstract).
- Cheng, B., Chen, F., and Zhang, J.: Palaeovegetational and palaeoenvironmental changes since the last deglacial in Gonghe Basin, northeast Tibetan Plateau, *J. Geogr. Sci.* 23, 136–146, <https://doi.org/10.1007/s11442-013-0999-5>, 2013.
- Chevalier, M., Davis, B. A. S., Heiri, O., Seppä, H., Chase, B. M., Gajewski, K., Lacourse, T., Telford, R. J., Finsinger, W., Guiot, J., Kühl, N., Maezumi, S. Y., Tipton, J. R., Carter, V. A., Brussel, T., Phelps, L. N., Dawson, A., Zanon, M., Vallé, F., Nolan, C., Mauri, A., de Vernal, A., Izumi, K., Holmström, L., Marsicek, J., Goring, S., Sommer, P. S., Chaput, M., and Kupriyanov, D.: Pollen-based climate reconstruction techniques for late Quaternary studies, *Earth-Sci. Rev.* 210, 103384,

- <https://doi.org/10.1016/j.earscirev.2020.103384>, 2020.
- ~~Ding, Z. L., Derbyshire, E., Yang, S. L., Sun, J. M., and Liu, T. S.: Stepwise expansion of desert environment across northern China in the past 3.5 Ma and implications for monsoon evolution, Earth Planet. Sci. Lett., 237, 45–55. <https://doi.org/10.1016/j.epsl.2005.06.036>, 2005.~~
- ~~Du, Y.: Land cover of Tibet Plateau (2015), National Tibetan Plateau Data Center, 2019.~~
- ~~Duan, R., Wei, H., Hou, G., Gao, J., Du, Y., and Qin, Z.: Modern Pollen Assemblages in Typical Agro-Pastoral Ecotone in the Eastern Tibetan Plateau and Its Implications for Anthropogenic Activities, Front. Ecol. Evol., 9, 685942. <https://doi.org/10.3389/fevo.2021.685942>, 2021.~~
- Duan, Y., Zhao, Y., Wu, Y., He, J., Xu, L., Zhang, X., Ma, L., and Qian, R.: δD values of n-alkanes in sediments from Gahai Lake, Gannan, China: implications for sources of organic matter, J. Paleolimnol., 56, 95–107, <https://doi.org/10.1007/s10933-016-9895-1>, 2016.
- Dykoski, C. A., Edwards, R. L., Cheng, H., Yuan, D. X., Cai, Y., Zhang, M., Lin, Y., Qing, J., An, Z., and Revenaugh, J.: A high-resolution, absolute-dated Holocene and deglacial Asian monsoon record from Dongge Cave, China, Earth Planet. Sci. Lett., 233, 71–86, <https://doi.org/10.1016/j.epsl.2005.01.036>, 2005.
- ~~Fan, Q., Ma, H., Wei, H., and An, F.: Holocene lake level changes of Hurleg Lake on northeastern Qinghai-Tibetan Plateau and possible forcing mechanism, Holocene, 24, 274–283, doi:10.1177/0959683613517399, 2014.~~
- Fægri, K., and Iversen, J.: Textbook of pollen analysis, Munksgaard, Copenhagen, 1975.
- ~~Folk, R. L., and Ward, W. C.: Brazos River bar: a study in the significance of grain size parameters, J. Sediment. Petrol., 27, 3–26, <https://doi.org/10.1306/74D70646-2B21-11D7-8648000102C1865D>, 1957.~~
- ~~Håkanson, L., and Jansson, M.: Principles of Lake Sedimentology, Springer, 316 pp., Verlag, Berlin, 1983.~~
- Herzschuh, U.: Reliability of pollen ratios for environmental reconstructions on the

-
- Tibetan Plateau, *J. Biogeogr.*, 34, 1265–1273, <https://doi.org/10.1111/j.1365-2699.2006.01680.x>, 2007.
- Herzschuh, U., Birks, H. J. B., Mischke, S., Zhang, C., and Böhner, J.: A modern pollen-climate calibration set based on lake sediments from the Tibetan Plateau and its application to a Late Quaternary pollen record from the Qilian Mountains, *J. Biogeogr.*, 37, 752–766, <https://doi.org/10.1111/j.1365-2699.2009.02245.x>, 2010.
- Herzschuh, U., Borkowski, J., Schewe, J., Mischke, S., and Tian, F.: Moisture advection feedback supports strong early-to-mid Holocene monsoon climate on the eastern Tibetan Plateau as inferred from a pollen-based reconstruction, *Paleogeogr. Paleoclimatol. Paleoecol.*, 402, 44–54, <https://doi.org/10.1016/j.palaeo.2014.02.022>, 2014.
- Herzschuh, U., Kramer, A., Mischke, S., and Zhang, C.: Quantitative climate and vegetation trends since the late glacial on the north-east Tibetan Plateau deduced from Koucha Lake pollen spectra, *Quat. Res.*, 71, 162–171, <https://doi.org/10.1016/j.yqres.2008.09.003>, 2009.
- Herzschuh, U., Kürschner, H., and Mischke, S.: Temperature variability and vertical vegetation belt shifts during the last ~50,000 yr in the Qilian Mountains (NE margin of the Tibetan Plateau, China), *Quat. Res.*, 66, 133–146, <https://doi.org/10.1016/j.yqres.2006.03.001>, 2006.
- ~~Herzschuh, U., Winter, K., Wünnemann, B., and Li, S.: A general cooling trend on the central Tibetan Plateau throughout the Holocene recorded by the Lake Zigetang pollen spectra, *Quat. Int.*, 154–155, 113–121, doi: 10.1016/j.quaint.2006.02.005, 2006.~~
- Herzschuh, U., Zhang, C., Mischke, S., Herzschuh, R., Mohammadi, F., Mingram, B., Kürschner, H., and Riedel, F.: A late Quaternary lake record from the Qilian Mountains (NW China), evolution of the primary production and the water depth reconstructed from macrofossil, pollen, biomarker and isotope data, *Global Planet. Change*, 46, 361–379, <https://doi.org/10.1016/j.gloplacha.2004.09.024>, 2005.
- Hill, M. O., and Gauch, H. G.: Detrended correspondence analysis: an improved

ordination technique, *Vegetatio*, 42, 41–58, <https://doi.org/10.1007/BF00048870>, 1980.

Huang, X., ~~Liu, S., Dong, G., Qiang, M., Bai, Z., Zhao, Y., and Chen, F.:~~ Early human impacts on vegetation on the north-east Qinghai-Tibetan Plateau during the middle to late Holocene. *Prog. Phys. Geogr.* 41, 1–16, doi: 10.1177/0309133317703035, 2017.

~~Huang, X.,~~ Peng, W., Rudaya, N., Grimm, E. C., Chen, X., Cao, X., Zhang, J., Pan, X., Liu, S., Chen, C., and Chen, F.: Holocene Vegetation and Climate Dynamics in the Altai Mountains and Surrounding Areas, *Geophys. Res. Lett.*, 45, 6628–6636. <https://doi.org/10.1029/2018GL078028>, 2018

Ji, J., Shen, J., Balsam, W., Chen, J., Liu, L., and Liu, X.: Asian monsoon oscillations in the north-east Qinghai-Tibet Plateau since the late glacial as interpreted from visible reflectance of Qinghai Lake sediments, *Earth Planet. Sci. Lett.*, 233, 61–70, <https://doi.org/10.1016/j.epsl.2005.02.025>, 2005.

Juggins, S., ~~2012. Rioja: analysis.:~~ rioja: Analysis of Quaternary ~~science data~~ Science Data, version 0.7-3. ~~Available~~ 9-26, available at: <http://cran.r-project.org/web/packages/rioja/index.html>.

~~Juggins, S., and Birks, H. J. B.: Quantitative environmental reconstructions from biological data, in: Birks, H. J. B., Lotter, A. F., Juggins, S., and Smol, J. P., Tracking environmental change using lake sediments (vol. 5): Data handling and numerical techniques, Springer, Netherlands, 431–494, doi: 10.1007/978-94-007-2745-8, 2012~~ <https://CRAN.R-project.org/package=rioja>, 2020.

Kasper, T., Haberzettl, T., Wang, J., Daut, G., Doberschütz, S., Zhu, L., and Mäusbacher, R.: Hydrological variations on the Central Tibetan Plateau since the LGM and their teleconnections to inter-regional and hemispheric climate variations, *J. Quat. Sci.*, 30, 70–78, <https://doi.org/10.1002/jqs.2759>, 2015.

~~Kramer, A., Herzschuh, U., Mischke, S., and Zhang, C.: Holocene tree-line shifts and monsoon variability in the Hengduan Mountains (south-eastern Tibetan Plateau) implications from palynological investigations. *Palaeogeogr. Palaeoclimatol.*~~

- ~~Palaeocol.~~ 286, 23–41, doi: 10.1016/j.palaeo.2009.12.001, 2010a.
- Kramer, A., Herzsuh, U., Mischke, S., and Zhang, C.: Late Glacial vegetation and climate oscillations on the south-eastern Tibetan Plateau inferred from the Lake Naleng pollen profile, *Quat. Res.*, 73, 324–335, <https://doi.org/10.1016/j.yqres.2009.12.003>, 2010b, 2010.
- Li, Y., Yu, G., Shen, H., Hu, S., Yao, S., and Yin, G.: Study on lacustrine sediments responding to climatic precipitation and flood discharge in Lake Taihu catchment, China. *Acta Sediment. Sin.*, 30, 1099–1105, 2012. (in Chinese with English abstract)
- ~~Li, K., Liao, M., Ni, J., Liu, X., and Wang, Y.: Treeline composition and biodiversity change on the southeastern Tibetan plateau during the past millennium, inferred from a high-resolution alpine pollen record. *Quat. Sci. Rev.*, 206, 44–55, doi: 10.1016/j.quascirev.2018.12.029, 2019.~~
- ~~Li, Q., Ge, Q., and Tong, G.: Modern pollen-vegetation relationship based on discriminant analysis across an altitudinal transect on Gongga Mountain, eastern Tibetan Plateau, *Chin. Sci. Bull.*, 57, 4600–4608, doi: 10.1007/s11434-012-5236-6, 2012.~~
- ~~Li, Y., Qiang, M., Huang, X., Zhao, Y., Leppänen, J. J., Weckström, J., and Välimäki, M.: Lateglacial and Holocene climate change in the NE Tibetan Plateau: Reconciling divergent proxies of Asian summer monsoon variability. *Catena*, 199, 105089, doi: 10.1016/j.catena.2020.105089, 2021.~~
- ~~Liang, C., Zhao, Y., Qin, F., Zheng, Z., Xiao, X., Ma, C., Li, H., and Zhao, W.: Pollen-based Holocene Quantitative Temperature Reconstruction on the Eastern Tibetan Plateau Using a Comprehensive Method Framework, *Sci. China. Earth. Sci.*, 63, 1144–1160, doi: 10.1007/s11430-019-9599-y, 2020.~~
- Liang, W.: Luqu County Annals, Gansu Culture Press, Lanzhou, 2006. (in Chinese)
- Lin, L., Zhang, D., Cao, G., Ouyang, J., Ke, X., Liu, S., Liu, S., Kruse, S., Scherler, D., Ree, R. H., Zimmermann, H. H., Stoof-Leichsenring, K. R., Epp, L. S., Mischke, S., and Herzsuh, U.: Sedimentary ancient DNA reveals a threat of warming-induced alpine habitat loss to Tibetan Plateau plant diversity, *Nat.*

- ~~Commun., 12, 2995, doi: 10.1038/s41467-021-22986-4, 2021.~~
- Zhang, F., Li, Y., and Guo, X.: Responses of soil nutrient traits to grazing intensities in alpine Kobresia meadows, Acta Ecol. Sin., 36, 4664-4671, 2016 (in Chinese with English abstract)
- Liu, X., Lai Z., Madsen, D., and Zeng, F.: Last deglacial and Holocene lake level variations of Qinghai Lake, north-east Qinghai-Tibetan Plateau, J. Quat. Sci., 30, 245-257, <https://doi.org/10.1002/jqs.2777>, 2015.
- Liu, X., Herzschuh, U., Shen, J., Jiang, Q., and Xiao, X.: Holocene environmental and climatic changes inferred from Wulungu Lake in northern Xinjiang, China, Quat. Res., 70, 412–425, <https://doi.org/10.1016/j.yqres.2008.06.005>, 2008.
- Liu, X., Vandenberghe, J., An, Z., Li, Y., Jin, Z., Dong, J., and Sun, Y.: Grain size of Lake Qinghai sediments: implications for riverine input and Holocene monsoon variability, Palaeogeogr. Palaeoclimatol. Palaeoecol., 449, 41–51, <https://doi.org/10.1016/j.palaeo.2016.02.005>, 2016.
- ~~Lowe, J. J., and Walker, M. J. C.: Reconstructing Quaternary Environments, Harlow: Longman, 1–472, 1997.~~
- Lu, H., Wang, S., Shen, C., Yang, X., Tong, G., and Liao, G.: Spatial pattern of modern *Abies* and *Picea* pollen in the Qinghai-Xizang Plateau, Quat. Sci., 24, 39–49, 2004 (in Chinese with English abstract).
- Lu, H., Wu, N., Liu, K.-B., Zhu, L., Yang, X., Yao, T., Wang, L., Li, Q., Liu, X., Shen, C., Li, X., Tong, G., and Jiang, H.: Modern pollen distributions in Qinghai-Tibetan Plateau and the development of transfer functions for reconstructing Holocene environmental changes, Quat. Sci. Rev., Luo, C., Zheng, Z., Tarasov, P., Pan, A., Huang, K. Y., Beaudouin, C., and An, F.: Characteristics of the modern pollen distribution and their relationship to vegetation in the Xinjiang region, northwestern China, Rev. 30, 947–966, <https://doi.org/10.1016/j.quascirev.2011.01.008>, 2011.
- ~~Palaeobot. Palynol. 153, 282–295, doi: 10.1016/j.revpalbo.2008.08.007, 2009.~~
- Ma, Q., Zhu, L., Lü, X., Wang, J., Ju, J., Kasper, T., Daut, G., and Haberzettl, T.: Late glacial and Holocene vegetation and climate variations at Lake Tangra Yumco,

- central Tibetan Plateau, *Global Planet. Change.*, 174, 16–25,
<https://doi.org/10.1016/j.gloplacha.2019.01.004>, 2019a2019.
- Ma, Q., Zhu, L., Lu, X., Wang, Y., Guo, Y., Wang, J., Ju, J., Peng, P., and Tang, L.:
Modern pollen assemblages from surface lake sediments and their environmental
implications on the southwestern Tibetan Plateau, *Boreas*, 46, 242–253,
<https://doi.org/10.1111/bor.12201>, 2017.
- ~~Ma, Q., Zhu, L., Wang, J., Ju, J., Wang, Y., Lü, X., Kasper, T., and Haberzettl, T.: Late
Holocene vegetation responses to climate change and human impact on the central
Tibetan Plateau, *Sci. Total Environ.* 708, 135370, doi:
10.1016/j.scitotenv.2019.135370, 2019b.~~
- ~~Ma, R., Yang, G., Duan, H., Jiang, J., Wang, S., Feng, X., Li, A., Kong, F., Xue, B.,
Wu, J., and Li, S.: China's lakes at present: Number, area and spatial distribution,
Sci. China Earth. Sci., 54, 283–289, doi: 10.1007/s11430-010-4052-6, 2011.~~
- Ma, Y., Liu, K. -B., Feng, Z., Sang, Y., Wang, W., and Sun, A.: A survey of modern
pollen and vegetation along a south–north transect in Mongolia, *J. Biogeogr.*, 35,
1512–1532, <https://doi.org/10.1111/j.1365-2699.2007.01871.x>, 2008.
- Meyers, P. A.: Applications of organic geochemistry to paleolimnological
reconstructions: a summary of examples from the Laurentian Great Lakes, *Org.
Geochem.*, 34, 261–289, [https://doi.org/10.1016/S0146-6380\(02\)00168-7](https://doi.org/10.1016/S0146-6380(02)00168-7), 2003.
- Meyers, P. A., and Ishiwatari, R.: Lacustrine organic geochemistry – an overview of
indicators of organic matter sources and diagenesis in lake sediments. *Org.
Geochem.*, 20, 867–900, [https://doi.org/10.1016/0146-6380\(93\)90100-P](https://doi.org/10.1016/0146-6380(93)90100-P), 1993.
- ~~Miehe, G., Miehe, S., Böhner, J., Kaiser, K., Hensen, I., Madsen, D., Liu, J., and
Opgenoorth, L.: How old is the human footprint in the world's largest alpine
ecosystem? A review of multiproxy records from the Tibetan Plateau from the
ecologists' viewpoint, *Quat. Sci. Rev.*, 86, 190–209,
<https://doi.org/10.1016/j.quascirev.2013.12.004>, 2014.~~
- Mykleby, P. M., Snyder, P. K., and Twine, T. E.: Quantifying the trade-off between
carbon sequestration and albedo in midlatitude and high-latitude North American

forests, *Geophys. Res. Lett.*, **44**, 2493–2501,
<https://doi.org/10.1002/2016gl071459>, 2017.

Nychka, D., Furrer, R., Paige, J., and Sain, S.: *fields: Tools for spatial data*, version 13.3, available at: <https://github.com/dnychka/fieldsRPackage>, 2021.

Oksanen, J., Blanchet, F. G., Friendly, M., Kindt, R., Legendre, P., McGlinn, D., Minchin, P. R., O’Hara, R. B., Simpson, G. L., Solymos, P., Stevens, M. H. H., Szoecs, E., and Wagner, H.: *vegan: Community Ecology Package*, version 2.5-4, available at: <https://cran.r-project.org/web/packages/vegan/index.html> (last access: June 2020), 2019.

Opitz, S., Wünnemann, B., Aichner, B., Dietze, E., Hartmann, K., Herzsuh, U., Uecker, J., Lehmkuhl, F., Li, S., Mischke, S., Plotzki, A., Stauch, G., Diekmann, B.: Late Glacial and Holocene development of Lake Donggi Cona, north-eastern Tibetan Plateau, inferred from sedimentological analysis, *Palaeogeogr. Palaeoclimatol. Palaeoecol.*, **337**, 159–176, <https://doi.org/10.1016/j.palaeo.2012.04.013>, 2012.

Ota, Y., Kawahata, H., Sato, T., and Seto, K.: Flooding history of Lake Nakaumi, western Japan, inferred from sediment records spanning the past 700 years, *J. Quat. Sci.*, **32**, 1063–1074, <https://doi.org/10.1002/jqs.2982>, 2017.

Peng, Y., Xiao, J., Nakamura, T., Liu, B., and Inouchi, Y.: Holocene East Asian monsoonal precipitation pattern revealed by grain-size distribution of core sediments of Daihai Lake in Inner Mongolia of north-central China, *Earth Planet. Sci. Lett.*, **233**, 467–479, <https://doi.org/10.1016/j.epsl.2005.02.022>, 2005.

Prentice, I. C.: Multidimensional scaling as a research tool in Quaternary palynology: a review of theory and methods, *Rev. Palaeobot. Palynol.*, **31**, 71–104, [https://doi.org/10.1016/0034-6667\(80\)90023-8](https://doi.org/10.1016/0034-6667(80)90023-8), 1980.

Qiang, M., Liu, Y., Jin, Y., Song, L., Huang, X., and Chen, F.: Holocene record of eolian activity from Genggahai Lake, north-east Qinghai-Tibetan plateau, China, *Geophys. Res. Lett.*, **41**, 589–595, <https://doi.org/10.1002/2013GL058806>, 2014.

Qiang, M., Song, L., Chen, F., Li, M., Liu, X., and Wang, Q.: A 16-ka lake-level

record inferred from macrofossils in a sediment core from Genggahai Lake, north-east Qinghai-Tibetan Plateau (China), *J. Paleolimnol.*, 49, 575–590, <https://doi.org/10.1007/s10933-012-9660-z>, 2013.

Qin, F.: Modern pollen assemblages of the surface lake sediments from the steppe and desert zones of the Tibetan Plateau, *Sci. China Earth Sci.*, 64, 425–439, <https://doi.org/10.1007/s11430-020-9693-y>, 2021.

R Core Team, 2021. R, A language and environment for statistical computing, R Foundation for Statistical Computing, Vienna.

Reimer, P. J., Austin, W. E. N., Bard, E., Bayliss, A., Blackwell, P. G., Bronk Ramsey, C., Butzin, M., Cheng, H., Edwards, R. L., Friedrich, M., Grootes, P. M., Guilderson, T. P., Hajdas, I., Heaton, T. J., Hogg, A. G., Hughen, K. A., Kromer, B., Manning, S. W., Muscheler, R., Palmer, J. G., Pearson, C., Van Der Plicht, J., Reimer, R. W., Richards, D. A., Scott, E. M., Southon, J. R., Turney, C. S. M., Wacker, L., Adolphi, F., Büntgen, U., Capano, M., Fahrni, S. M., Fogtmann-Schulz, A., Friedrich, R., Köhler, P., Kudsk, S., Miyake, F., Olsen, J., Reinig, F., Sakamoto, M., Sookdeo, A., and Talamo, S.: The IntCal20 Northern Hemisphere Radiocarbon Age Calibration Curve (0-55 cal kBP), *Radiocarbon*, 62, 725–757, <https://doi.org/10.1017/RDC.2020.41>, 2020.

~~Schlütz, F., and Lehmkuhl, F.: Holocene climatic change and the nomadic Anthropocene in Eastern Tibet: palynological and geomorphological results from the Nianbaoyeze Mountains, *Quat. Sci. Rev.*, 28, 1449–1471, doi: 10.1016/j.quascirev.2009.01.009, 2009.~~

Shen, C., Liu, K., Tang, L., and Overpeck, J.: Modern pollen rain in the Tibetan Plateau, *Front. Earth Sci.*, 9, 732441, <https://doi.org/10.3389/feart.2021.732441>, 2021.

Shen, J., Liu, X. Q., Wang, S. M., and Matsumoto, R.: Palaeoclimatic changes in the Qinghai Lake area during the last 18,000 years, *Quat. Int.*, 136, 131–140, <https://doi.org/10.1016/j.quaint.2004.11.014>, 2005.

Sun, X., Zhao, Y., and Li, Q.: Holocene peatland development and vegetation changes

- in the Zoige Basin, eastern Tibetan Plateau, *Sci. China Earth Sci.*, 47, 1097–1109,
<https://doi.org/10.1007/s11430-017-9086-5>, 2017.
- Tang, L., Mao, L., Shu, J., Li, C., Shen, C., and Zhou, Z.: An Illustrated Handbook of
 Quaternary Pollen and Spores in China. Science Press, Beijing, 2017. ~~(In Chinese
 with English summary)~~
- ter Braak, C. J. F., and Verdonschot, P. F. M.: Canonical correspondence analysis and
 related multivariate methods in aquatic ecology, *Aquat. Sci.*, 57, 255–289,
<https://doi.org/10.1007/BF00877430>, 1995.
- ter Braak, C. J. F., and Prentice, I. C.: A theory of gradient analysis, *Adv. Ecol. Res.*,
 18, 271–317, [https://doi.org/10.1016/S0065-2504\(08\)60183-X](https://doi.org/10.1016/S0065-2504(08)60183-X), 1988.
- Wang, F.-X., Qian, N.-F., Zhang, Y.-L., and Yang, H.-Q.: Pollen Flora of China.
 Science Press, Beijing, 1995. (In Chinese)
- Wang, H., Hu, Y., Zhang, X., Lv, F., Ma, X., W, D., Chen, F., Zhou, A., Hou, J., and
 Chen, J.: A 17 ka multi-proxy paleoclimatic record on the north-east Tibetan
 Plateau: implications for the northernmost boundary of the Asian summer monsoon
 during the Holocene, *Int. J. Climatol.*, 42, 191–201,
<https://doi.org/10.1002/joc.7239>, 2021.
- Wang, N., Liu, L., Zhang, Y., and Cao, X.: A modern pollen data set for the forest–
 meadow–steppe ecotone from the Tibetan Plateau and its potential use in past
 vegetation reconstruction. *Boreas*, <https://doi.org/10.1111/bor.12589>, 2022.
- Wang, X., Yi, S., Lu, H., Vandenberghe, J., and Han, Z.: Aeolian process and climatic
 changes in loess recorded from the NTP: response to global temperature forcing
 since 30 ka. ~~*Paleoceanogr. Paleoclim.*~~ *Paleoceanography*, 30, 612–620,
<https://doi.org/10.1002/2014PA002731>, 2015.
- Wang, Y., Herzschuh, U., Shumilovskikh, L., Mischke, S., Birks, H. J. B.,
 Wischniewski, J., Böhner, J., Schlütz, F., Lehmkuhl, F., Diekmann, B., Wünnemann,
 B., and Zhang, C.: Quantitative reconstruction of precipitation changes on the NE
 Tibetan Plateau since the Last Glacial Maximum – extending the concept of pollen
 source area to pollen-based climate reconstructions from large lakes, *Clim. Past.*,

- 10, 21–39, <https://doi.org/10.5194/cp-10-21-2014>, 2014.
- Wang, Y., Cheng, H., Edwards, R. L., An, Z., Wu, J., Shen, C., and Dorale, J. A.: A high-resolution absolute-dated Late Pleistocene monsoon record from Hulu Cave, China, *Science*, 294, 2345–2348, <https://doi.org/10.1126/science.1064618>, 2001.
- Wei, H., ~~Ma, C., Zhang, J., Sun, Y., LiYuan, Q., Hou, G Xu, Q., Qin, Z., Wang, L., Fan, Q., and Duan, R.: Climate change and anthropogenic~~Shan, F.: Assessing the impact of human activities on surface pollen assemblages in Qinghai Lake ~~basin over the last 8500 years derived from pollen and charcoal records in an aeolian section, Catena, 193, 104616, Basin, China, J. Quaternary Sci., 33, 702–712, https://doi.org/10.1016/j.catena.2020.104616, 20201002/jqs.3046, 2018.~~
- Wischnewski, J., Mischke, S., Wang, Y., and Herzschuh, U.: Reconstructing climate variability on the north-east Tibetan Plateau since the last Lateglacial—a multi proxy, dual-site approach comparing terrestrial and aquatic signals, *Quat. Sci. Rev.*, 30, 82–97, <https://doi.org/10.1016/j.quascirev.2010.10.001>, 2011.
- Xiao, J., Fan, J., Zhou, L., Zhai, D., Wen, R., and Qin, X.: A model for linking grain-size component to lake level status of a modern clastic lake. *J. Asian Earth Sci.*, 69, 149–158, <https://doi.org/10.1016/j.jseaes.2012.07.003>, 2013.
- Xu, D., Lu, H., Wu, N., Liu, Z., Li, T., Shen, C., and Wang, L.: Asynchronous marine-terrestrial signals of the last deglacial warming in East Asia associated with low- and high-latitude climate changes, *Proc. Natl. Acad. Sci. USA.*, 110, 9657–9662, <https://doi.org/10.1073/pnas.1300025110>, 2013.
- Xu, Q., Li, Y., Yang, X., and Zheng, Z.: Quantitative relationship between pollen and vegetation in northern China, *Sci. China Ser. D-Earth. Sci.*, 50, 582–599, <https://doi.org/10.1007/s11430-007-2044-y>, 2007.
- Yan, D., and Wünnemann, B.: Late Quaternary water depth changes in Hala Lake, northeastern Tibetan Plateau, derived from ostracod assemblages and sediment properties in multiple sediment records, *Quat. Sci. Rev.*, 95, 95–114, <https://doi.org/10.1016/j.quascirev.2014.04.030>, 2014.
- ~~Yang B., Tang L., Brauning, A., Davis, M. E., Shao, J., and Liu, J.: Summer~~

- ~~temperature reconstruction on the central Tibetan Plateau during 1860–2002 derived from ice core pollen, *J. Geophys. Res. Atmos.*, 113, doi: 10.1029/2008JD010142, 2008.~~
- ~~Yao, Z.: Ice core pollen studies from the Dunde and Guliya Ice Caps, Qinghai-Tibetan Plateau, China, PhD Dissertation, Baton Rouge: Louisiana State University, USA, 2000.~~
- Yu, G., Tang, L., Yang, X., Ke, X., and Harrison, S. P.: Modern Pollen Samples from Alpine Vegetation on the Tibetan Plateau. *Global Ecol. Biogeogr.*, 10, 503–519, <https://doi.org/10.1046/j.1466-822x.2001.00258.x>, 2001.
- ~~Zhao, Y., and Herzschuh, U.: Modern pollen representation of source vegetation in the Qaidam Basin and surrounding mountains, north-eastern Tibetan Plateau, *Veget. Hist. Archaeobot.*, 18, 245–260, doi: 10.1007/s00334-008-0201-7, 2009.~~
- ~~Yuan, J., Jiang, X., Huang, W., and Wang, G: Effects of grazing intensity and grazing season on plant species diversity in alpine meadow, *Acta Pratac. Sin.*, 13, 16–21, 2004. (in Chinese with English abstract)~~
- Zhao, Y., Liu, Y., Guo, Z., Fang, K., Li, Q., and Cao, X.: Abrupt vegetation shifts caused by gradual climate changes in central Asia during the Holocene. *Sci. China Earth Sci.*, 60, 1317–1327, <https://doi.org/10.1007/s11430-017-9047-7>, 2017.
- ~~Zhao, Y., Tzedakis, P. C., Li, Q., Qin, F., Cui, Q., Liang, C., Birks, H. J. B., Liu, Y., Zhang, Z., Ge, J., Zhao, H., Felde, V. A., Deng, C., Cai, M., Li, H., Ren, W., Wei, H., Yang, H., Zhang, J., Yu, Z., and Guo, Z.: Evolution of vegetation and climate variability on the Tibetan Plateau over the past 1.74 million years, *Sci. Adv.*, 6, eaay6193, doi: 10.1126/sciadv.aay6193, 2020.~~
- Zhao, Y., Yu, Z., and Zhao, W.: Holocene vegetation and climate histories in the eastern Tibetan Plateau: controls by insolation-driven temperature or monsoon-derived precipitation changes? *Quat. Sci. Rev.*, 30, 1173–1184, <https://doi.org/10.1016/j.quascirev.2011.02.006>, 2011.
- Zhou, J., Wu, J., and Zeng, H.: Extreme flood events over the past 300 years inferred from lake sedimentary grain sizes in the Altay Mountains, northwestern China,

-
- ~~Chin. Geogra. Sci., Zhao, Y., Yu, Z., Chen, F., Ito, E., and Zhao, C.: Holocene vegetation and climate history at Hurleg Lake in the Qaidam Basin, northwest China, — Rev. — Palaeobot. — Palynol., — 145, — 275–288, — doi: 10.1016/j.revpalbo.2006.12.002, 2007.~~
- ~~28, 773–783. <https://doi.org/10.1007/s11769-018-0968-0>, 2018.~~
- Zhou, W., Yu, S., Burr, G. S., Kukla, G. J., Jull, A. J. T., Xian, F., Xiao, J., Colman, S. M., Yu, H., Liu, H., Liu, Z., and Kong, X.: Postglacial changes in the Asian summer monsoon system: A pollen record from the eastern margin of the Tibetan Plateau, *Boreas*, 39, 528–539, <https://doi.org/10.1111/j.1502-3885.2010.00150.x>, 2010.
- Zhu, L., Lü, X., Wang, J., Peng, P., Kasper, T., Daut, G., Haberzettl, T., Frenzel, P., Li, Q., Yang, R., Schwalb, A., and Mäusbacher, R.: Climate change on the Tibetan Plateau in response to shifting atmospheric circulation since the LGM, *Sci. Rep.*, 5, 13318, <https://doi.org/10.1038/srep13318>, 2015.

Appendix

Appendices

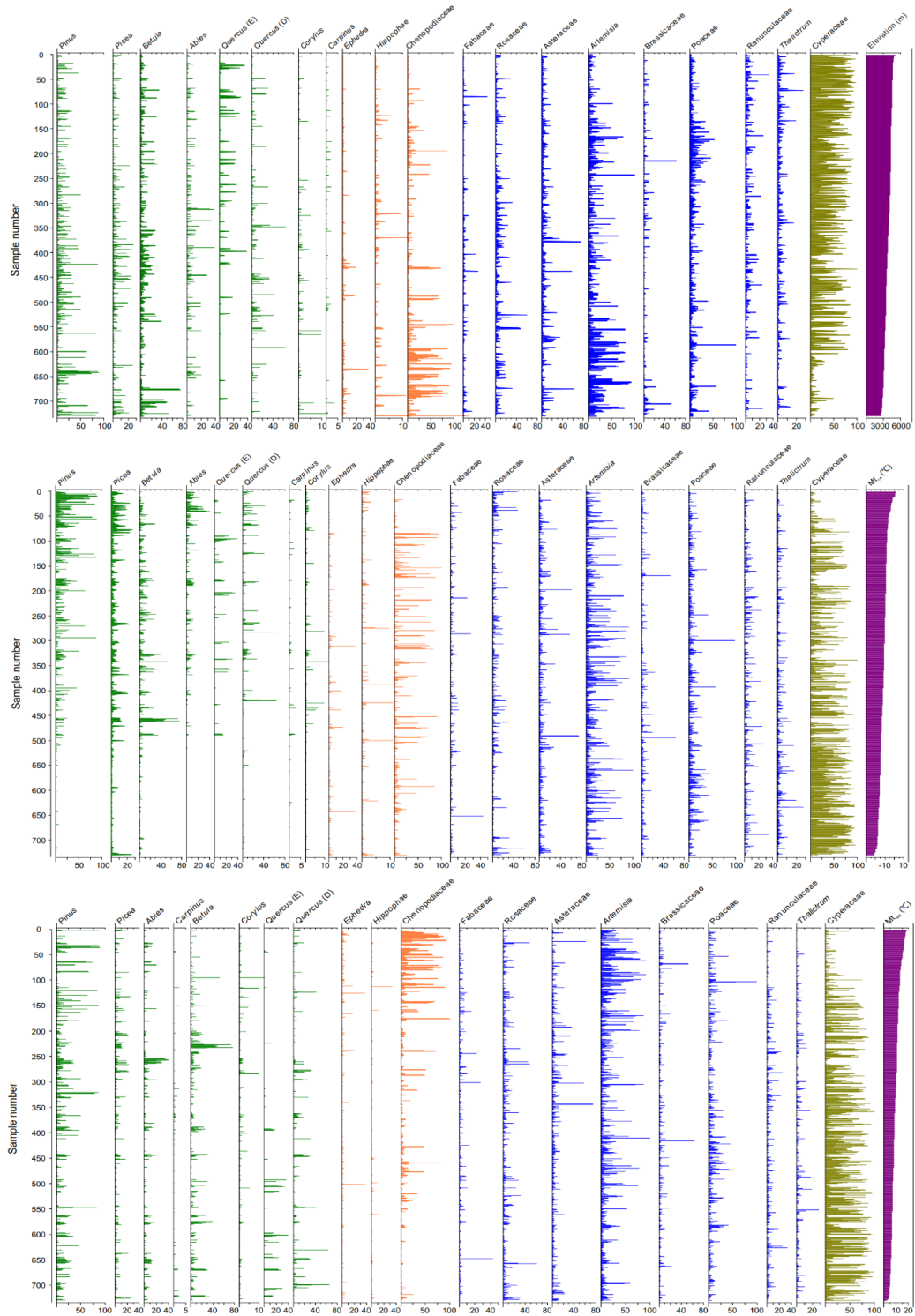


Figure A1. Pollen assemblages of the surface sediment samples with arranged along a

gradient of climate data (Elev, Mt_{co} , and Mt_{wa}) from the eastern Tibetan Plateau. Elev: Elevation (m); Mt_{co} : mean temperature of the coldest month ($^{\circ}\text{C}$); Mt_{wa} : mean temperature of the warmest month ($^{\circ}\text{C}$).

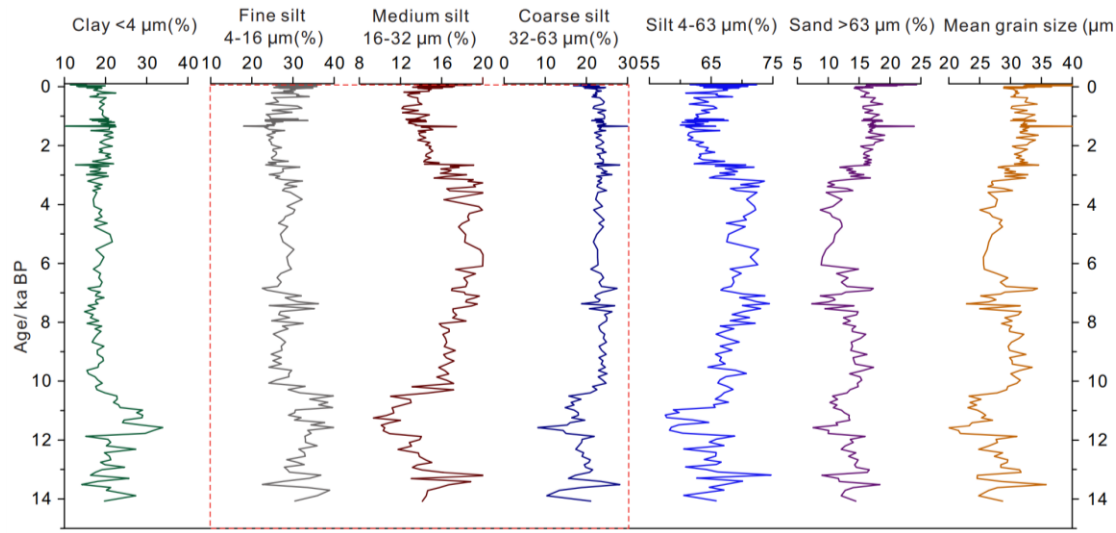


Figure A2. The percentage of different grain size components and mean grain size derived from Gahai Lake since 14.2 ka BP.

As noted in the main text, the silt fraction includes fine silt (4-16 μm), medium silt (16-32 μm), and coarse silt (32-63 μm). The proportions of the fine and coarse silt remain almost unchanged during the Holocene, while the medium silt fraction shows the most significant variation. In the sections below, we, therefore, use the whole silt fraction (4-63 μm) rather than the different grain sizes of silt fractions.

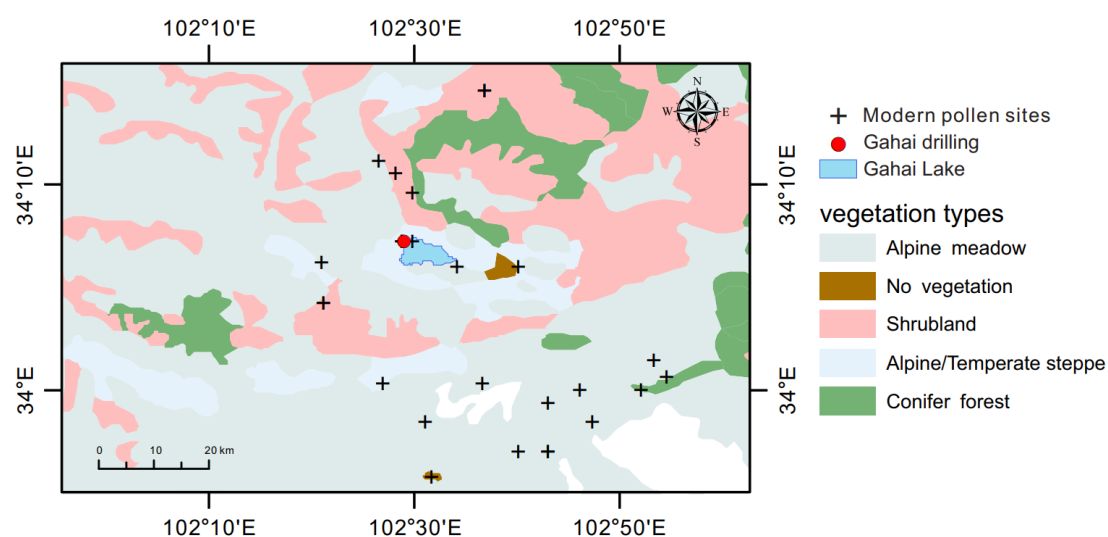


Figure A3. Location of the modern pollen samples (n=22) in the vicinity of Gahai Lake.

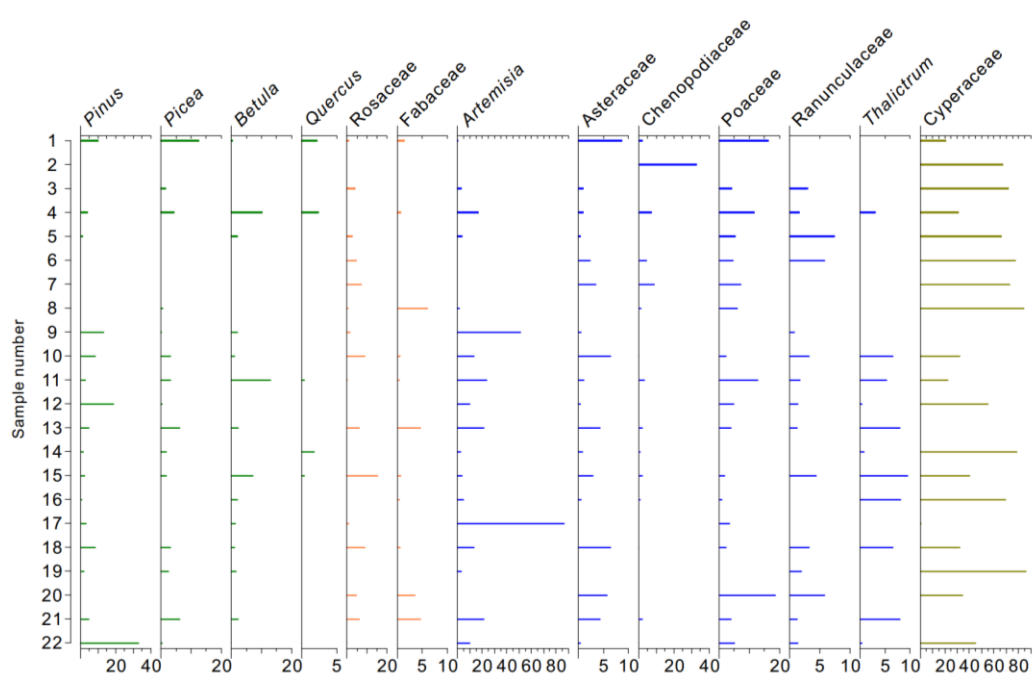


Figure A4. Pollen diagram of the modern pollen samples (n=22) in the vicinity of the Gahai Lake.